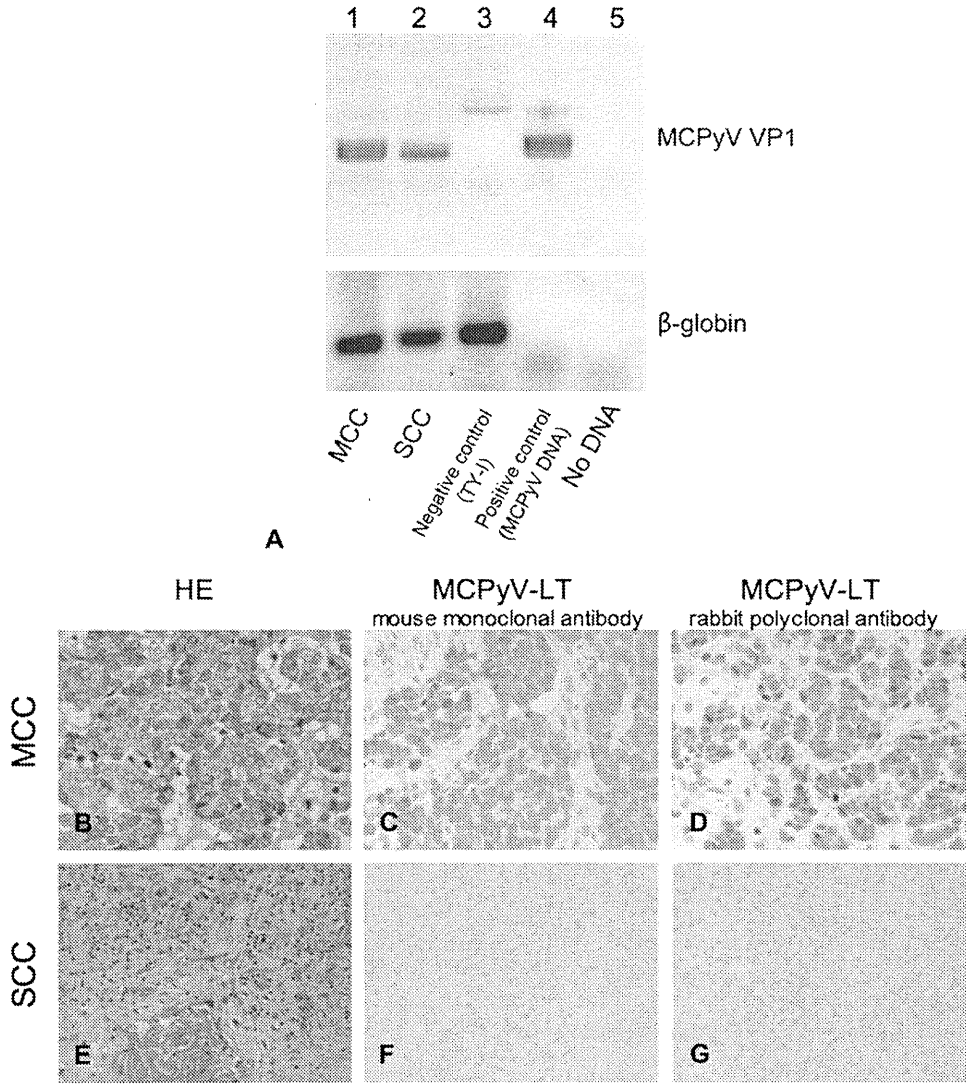

Fig 2. **A**, Detection of Merkel cell polyomavirus (*MCPyV*) by Southern blotting in polymerase chain reaction (PCR) products derived from Merkel cell carcinoma (*MCC*) and squamous cell carcinoma (*SCC*) lesions. Fragments of MCPyV were amplified by nested PCR from MCC lesions (lane 1) and SCC lesions (lane 2). Lower panel shows internal control PCR products of β-globin gene. **B** to **G**, Immunohistochemical detection of MCPyV-large tumor (*LT*) antigen in MCC and SCC lesions. Immunolabeling with mouse monoclonal antibody CM2B4 (**C**) and rabbit polyclonal antibody (**D**) detect LT antigen expression in diffuse nuclear pattern in tumor cells of MCC lesion. (Original magnification: ×400.) In contrast, tumor cells in SCC lesion show no MCPyV-LT antigen expression with CM2B4 (**F**) and rabbit polyclonal antibody (**G**) staining. (Original magnifications: ×400.) (**B** and **E**, Hematoxylin-eosin [*HE*] stain; original magnifications: ×400.)

positive for MCPyV-LT antigen, although the SCC cells were negative for it (Fig 2, *B* to *G*).

LT antigen is one of the tumor antigens encoded by MCPyV DNA. MCC cells frequently express this LT antigen in the nuclei.[3] Reisinger et al[4] reported that LT antigen was detected in 92% of MCC tumors from patients with secondary SCC or basal cell carcinoma. However, all the secondary non-MCC tumors were negative for LT antigen. Also in our case, LT antigen was positive only in the MCC, but negative in the SCC. On the other hand, our study revealed that MCPyV DNA was detected in SCC lesions that occurred before the MCC. Our results clearly indicate that the patient was infected with MCPyV at least 1 year before the occurrence of MCC, further attesting to the pathogenic role of MCPyV infection in MCC, although MCPyV has been found on the skin of

multiple healthy individuals with positive serologies.[5] The MCPyV copy number per cell in the SCC lesion was smaller than that in the MCC lesion. In addition, LT antigen was negative in the SCC lesion. Thus, we cannot conclude that MCPyV played a certain role in SCC oncogenesis in the current patient.

Kana Kaibuchi-Noda, MD,[a] Kenji Yokota, MD,[a] Takaaki Matsumoto, MD,[a] Masaki Sawada, MD,[a] Akihiro Sakakibara, MD, PhD,[a] Michihiro Kono, MD, PhD,[a] Yasushi Tomita, MD, PhD,[a] Daisuke Watanabe, MD, PhD,[b] Hitomi Fukumoto, MD,[c] Harutaka Katano, DDS, PhD,[c] and Masashi Akiyama, MD, PhD[a]

Department of Dermatology, Nagoya University Graduate School of Medicine[a]; Department of Dermatology, Aichi Medical University, Nagakute[b]; and Department of Pathology, National Institute of Infectious Diseases, Shinjuku, Tokyo[c]; Japan

Funding sources: None.

Conflicts of interest: None declared.

Correspondence to: Masashi Akiyama, MD, PhD, Department of Dermatology, Nagoya University Graduate School of Medicine, 65 Tsurumai-cho, Showa-ku, Nagoya, 466-8550 Japan

E-mail: makiyama@med.nagoya-u.ac.jp

REFERENCES

1. Feng H, Shuda M, Chang Y, Moore PS. Clonal integration of a polyomavirus in human Merkel cell carcinoma. Science 2008;319:1096-100.
2. Kassem A, Schöpfin A, Diaz C, Weyers W, Stickeler E, Werner M, et al. A frequent detection of Merkel cell polyomavirus in human Merkel cell carcinoma and identification of a unique deletion in the VP1 gene. Cancer Res 2008;68:5009-13.
3. Houben R, Shuda M, Weinkam R, Schrama D, Feng H, Chang Y, et al. Merkel cell polyomavirus-infected Merkel cell carcinoma cells require expression of viral T antigen. J Virol 2010;84: 7064-72.
4. Reisinger DM, Shiffer JD, Cognetta AB, Chang Y, Moore PS. Lack of evidence for basal or squamous cell carcinoma infection with Merkel cell polyomavirus in immunocompetent patients with Merkel cell carcinoma. J Am Acad Dermatol 2010;63:400-3.
5. Schowalter RM, Pastrana DV, Pumphrey KA, Moyer AL, Buck CB. Merkel cell polyomavirus and two previously unknown polyomaviruses are chronically shed from human skin. Cell Host Microbe 2010;7:509-15.

doi:10.1016/j.jaad.2011.06.026

Buyer beware: A black salve caution

To the Editor: Black salve ointments containing beeswax, cocoa butter, oil, charcoal, and clay have been used by the general public to treat boils, abscesses, bee stings, and other minor wounds. Other types of black salve products may also include zinc chloride or bloodroot extract (*Sanguinaria canadensis*), resulting in a biologically nonspecific corrosive escharotic agent capable of indiscriminately dissolving healthy and diseased tissue alike. Both types of products are advertised online as safe and effective for the treatment of more serious conditions, such as skin cancer, moles, warts, and skin tags. There are numerous testimonials online, but there are no scientific studies for clinical efficacy or safety. In addition, the wide diversity of poorly regulated black salve products, which often contain different ingredients and lack quality control, leads to confusion about the use of these products. We present a case that illustrates the danger of using poorly regulated online products perceived as safe and effective by the general public to treat serious dermatologic conditions.

A 63-year-old man had a history of an unknown neoplasm on his left naris. The neoplasm originally appeared in 1999 and, suspecting it to be a melanoma, he declined a biopsy and allopathic treatment, choosing rather to self-treat it with corrosive black salve product containing 300 mg of bloodroot, galangal, red clover, and sheep sorrel. After many months of treatment, the lesion resolved, however, extensive tissue damage imposed by the black salve product left the patient with an absent left naris (Figs 1 and 2).

In 2010, he returned with a hard, waxy nodule under his right eye. Biopsy specimen revealed a basal cell carcinoma. Despite his previous experience, the patient preferred to self-treat the lesion with the black salve product rather than have Mohs micrographic surgery. After a 4-month delay with no improvement, the patient reconsidered and consented to Mohs micrographic surgery. We could not determine if he would have had further recurrences, as a few months later, he was diagnosed with colon cancer and elected to self-treat this with oral black salve product and subsequently died.

The use of this black salve product resulted in severe skin damage. Histologic examination of tissues exposed to corrosive black salve products has shown extensive tissue necrosis with secondary necrotizing vasculitis.[1] Because of its escharotic character, corrosive black salve products may destroy both cancerous and healthy skin to a degree that eradicates the local cancer, but leaves an esthetically unpleasing result.[2] In addition, without a biopsy, there can be no guarantee the cancer has been completely eliminated. If residual cancer cells persist, the risk of recurrence and/or metastasis remains.[3,4] Self-treatment with black salve products

Disease Models & Mechanisms 4, 777-785 (2011) doi:10.1242/dmm.007146

RESEARCH ARTICLE

Abca12-mediated lipid transport and Snap29-dependent trafficking of lamellar granules are crucial for epidermal morphogenesis in a zebrafish model of ichthyosis

Qiaoli Li[1,*], Michael Frank[1,*], Masashi Akiyama[2,3], Hiroshi Shimizu[3], Shiu-Ying Ho[4], Christine Thisse[5], Bernard Thisse[5], Eli Sprecher[6] and Jouni Uitto[1,4,‡]

SUMMARY

Zebrafish (*Danio rerio*) can serve as a model system to study heritable skin diseases. The skin is rapidly developed during the first 5-6 days of embryonic growth, accompanied by expression of skin-specific genes. Transmission electron microscopy (TEM) of wild-type zebrafish at day 5 reveals a two-cell-layer epidermis separated from the underlying collagenous stroma by a basement membrane with fully developed hemidesmosomes. Scanning electron microscopy (SEM) reveals an ordered surface contour of keratinocytes with discrete microridges. To gain insight into epidermal morphogenesis, we have employed morpholino-mediated knockdown of the *abca12* and *snap29* genes, which are crucial for secretion of lipids and intracellular trafficking of lamellar granules, respectively. Morpholinos, when placed on exon-intron junctions, were >90% effective in preventing the corresponding gene expression when injected into one- to four-cell-stage embryos. By day 3, TEM of *abca12* morphants showed accumulation of lipid-containing electron-dense lamellar granules, whereas *snap29* morphants showed the presence of apparently empty vesicles in the epidermis. Evaluation of epidermal morphogenesis by SEM revealed similar perturbations in both cases in the microridge architecture and the development of spicule-like protrusions on the surface of keratinocytes. These morphological findings are akin to epidermal changes in harlequin ichthyosis and CEDNIK syndrome, autosomal recessive keratinization disorders due to mutations in the *ABCA12* and *SNAP29* genes, respectively. The results indicate that interference of independent pathways involving lipid transport in the epidermis can result in phenotypically similar perturbations in epidermal morphogenesis, and that these fish mutants can serve as a model to study the pathomechanisms of these keratinization disorders.

INTRODUCTION

Clinical and genetic heterogeneity of ichthyosis

Ichthyosis comprises a group of both acquired and heritable keratinization disorders characterized by hyperkeratotic and scaly skin (Brown and Irvine, 2008). Although the phenotypic spectrum of ichthyosiform dermatoses is extremely broad, with either limited or extensive involvement of the skin, among the inherited forms, three clinically and genetically distinct subtypes have been identified: ichthyosis vulgaris, X-linked ichthyosis and lamellar ichthyosis (LI) (McGrath and Uitto, 2008; Brown and Irvine, 2008; Brown and McLean, 2008; Elias et al., 2004). LI in itself is a heterogeneous group of autosomal recessive disorders with large plaque-like brown scales over most of the body, associated with ectropion and alopecia.

Harlequin ichthyosis (HI) is a rare, extremely severe form of ichthyosis, most closely associated with the LI group of these disorders (Akiyama, 2006a). Neonates are born encased in a thick skin that not only restricts their movement, but also distorts their facial features, averting their lips and eyelids. Although newborns with HI frequently die within the first few days of life, a few of these affected individuals do survive, and their skin eventually resembles severe non-bullous congenital ichthyosiform erythroderma or LI.

HI is an autosomal recessive disorder caused by mutations in the ATP-binding cassette, sub-family A, member 12 (*ABCA12*) gene, which encodes a lipid transporter protein localized to lamellar granules in epidermal keratinocytes (Sakai et al., 2007). Mutations in the *ABCA12* gene result in congested lipid secretion and impaired barrier function of the stratum corneum (Kelsell et al., 2005). Thus, *ABCA12* is crucial to the development of the skin-lipid barrier in the stratum corneum.

An *Abca12*$^{-/-}$ mouse model has been vital in confirming the role of this transporter molecule in the skin abnormalities seen in HI, i.e. hyperkeratosis, impaired barrier function, abnormal lamellar bodies and the retention of lipid droplets in the epidermis (Yanagi et al., 2008; Smyth et al., 2008; Sundberg et al., 1997). The role of Abca12 in transporting lipids was confirmed by culturing keratinocytes from *Abca12*$^{-/-}$ mice and observing impaired lipid

[1]Department of Dermatology and Cutaneous Biology, and [4]Department of Biochemistry and Molecular Biology, Jefferson Medical College, Thomas Jefferson University, Philadelphia, PA 19107, USA
[2]Department of Dermatology, Nagoya University Graduate School of Medicine, Nagoya 466-8550, Japan
[3]Department of Dermatology, Hokkaido University Graduate School of Medicine, Sapporo 060-8638, Japan
[5]Department of Cell Biology, University of Virginia School of Medicine, Charlottesville, VA 22908, USA
[6]Department of Dermatology, Tel Aviv Medical Center, Tel Aviv 64239, Israel
*These authors equally contributed to this work
‡Author for correspondence (Jouni.uitto@jefferson.edu)

Received 29 October 2010; Accepted 27 May 2011

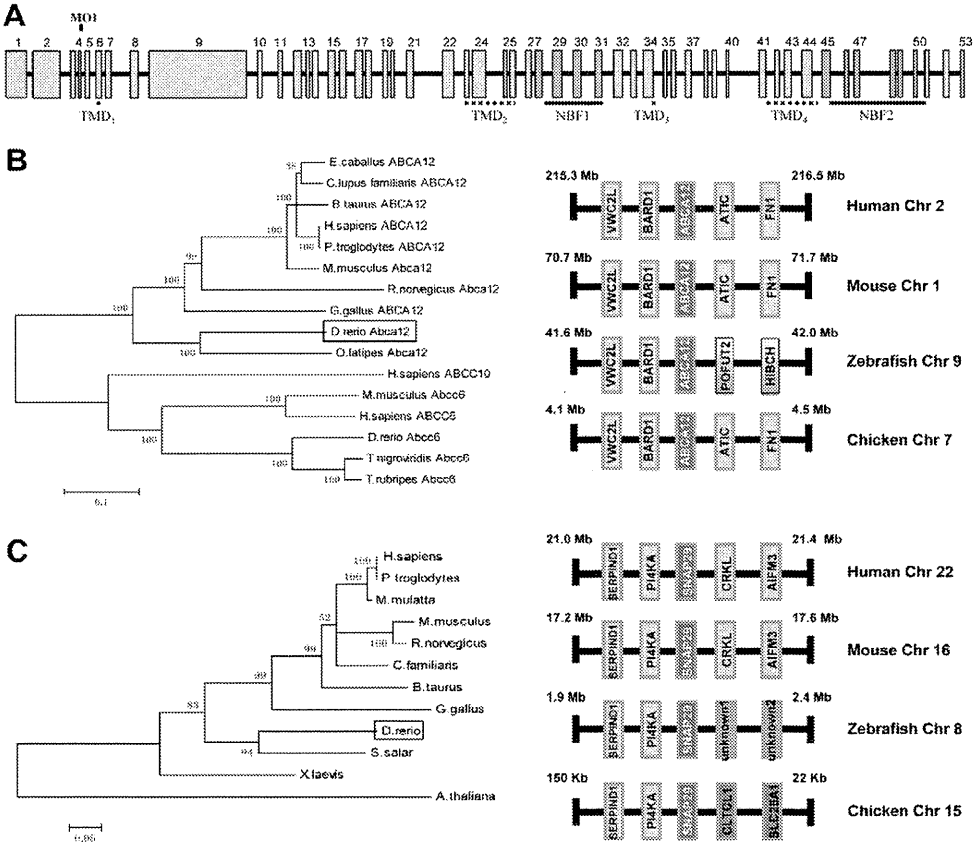

Fig. 1. Schematic representation of the zebrafish *abca12* gene, and the phylogenetic trees of the protein sequences of Abca12 and Snap29, together with syntenic analysis of the corresponding genes. (A) The *abca12* gene consists of 53 exons, which are numbered on the top, and the coding segments for transmembrane domains (TMDs) and nucleotide binding folds (NBFs; green) are underlined. Note the location corresponding to the morpholino (MO1) at the exon-4–intron-4 junction. (B) The phylogenetic relationship between zebrafish Abca12 and the other members of the ABC family of transporters estimated by the neighbor-joining method (left panel). The syntenic analysis of the *abca12* and flanking genes in human, mouse, zebrafish and chicken chromosomes is shown on right. (C) Cladogram and syntenic analysis of *snap29*. The unknown genes 1 and 2 in zebrafish chromosome 8 have been designated as si:dkey-178e17.1 and si:dkeyp-117b11.1, respectively.

efflux leading to intracellular accumulation of lipids, specifically ceramides (Akiyama et al., 2005). However, the drawback of the mouse model is the long gestation period and small number of offspring per litter.

In addition to nonsyndromic variants, ichthyosis can be associated with clinical manifestations in a number of organ systems besides the skin. An example of syndromic ichthyoses is the CEDNIK syndrome, a rare autosomal recessive disorder with cerebral dysgenesis, neuropathy, ichthyosis and keratoderma. This syndrome has been shown to be associated with mutations in the *SNAP29* gene, which encodes soluble n-ethylmaleimide sensitive factor (NSF) attachment protein (SNAP)29, a member of the SNAP receptor (SNARE) family of proteins (Sprecher et al., 2005; Fuchs-Telem et al., 2011). SNARE proteins are required for vesicle trafficking and they mediate the fusion between the vesicles and their target membranes. *SNAP29* deficiency has been suggested to result in impaired maturation and secretion of lamellar granules, particularly interfering with the transport of lipids to stratum corneum; however, no animal model for the CEDNIK syndrome exists.

In an attempt to create an alternative, and perhaps more expedient, model system to study ichthyosis, we have performed work on zebrafish (*Danio rerio*), which has nearly the same complement of genes as mammals. Some of the benefits to working with zebrafish include their rapid development and the ease with which one can manipulate their gene expression by morpholino-based antisense oligonucleotides (Kari et al., 2007; Li et al., 2011). Zebrafish develop rapidly, with all major organs, including the skin, having developed by 5-6 days post-fertilization (dpf). They also produce a large number of embryos per laying, approximately 50-100 per female. In this study, we performed experiments to show that *abca12* and *snap29* gene knockdown in zebrafish causes epidermal changes that are similar, attesting to the concept that diverse pathogenetic pathways, as a result of mutations in different genes, can result in phenotypes in the spectrum of ichthyotic diseases. Thus, zebrafish provide a novel and expedient model system to study this group of devastating, currently intractable, diseases.

RESULTS

Identification of an *ABCA12*-related gene in the zebrafish genome

Search of the online gene database (NCBI) identified one human *ABCA12*-related sequence, *abca12*, which mapped to zebrafish chromosome 9. This zebrafish *abca12* gene had an open reading frame, and all splice sites appeared intact, which allowed deduction of the intron-exon organization. The *abca12* gene consists of 53 exons, with sizes ranging from 55 to 2415 bp (Fig. 1A). The predicted primary sequence of the corresponding protein consists of 3634 amino acids, whereas the corresponding human primary sequence comprises 2595 amino acids. The overall conservation at the protein level was 49.3% and, consequently, the zebrafish *abca12* gene can be considered to be the human *ABCA12* homolog.

Alignment of human and zebrafish protein sequences revealed that zebrafish Abca12 has an extended 486 amino acid N-terminal sequence, as well as a number of insertions in the N-terminal half of the protein. However, alignment of zebrafish and human sequences identified conservation of domains that are characteristic of the ABC transporter proteins. Specifically, the zebrafish sequence, similar to the human sequence, was predicted to consist of four transmembrane domains (TMD1-4) and to contain two nucleotide binding fold domains (NBF1 and NBF2) (Tusnády et al., 2006) (Fig. 1A). The NBFs displayed characteristic sequences for Walker A and B motifs, as well as a highly conserved ABC signature sequence. Comparison of the deduced amino acid sequence within the NBF1 domain of zebrafish Abca12 showed 74% identity to the corresponding NBF1 domain in the human protein, whereas the NBF2 domain had 68% identity to human NBF2.

Evolutionary conservation of zebrafish *abca12*

Differences between the zebrafish *abca12* gene and homologous genes in other species were examined by phylogenetic analysis of the corresponding protein sequence by cladistic measurement (Fig. 1B). The cladogram suggested that the zebrafish gene is distant from most of the other *ABCA12*-related genes in a number of species, and, therefore, presumably diverged early. However, inclusion of other members of the ABC transporter family, such as ABCC10 and ABCC6, in different species, serving as an outgroup, indicated that the zebrafish Abca12 protein sequence is closer to human ABCA12 than it is to the sequences in the outgroup. To confirm that the zebrafish *abca12* is the correct ortholog of human *ABCA12*, syntenic analysis of *Abca12* in different species was performed (Fig. 1B). These analyses revealed that *ABCA12* and its flanking genes, *VWC2L* and *BARD1*, were located on the same chromosome in the same gene order in human, mouse, zebrafish and chicken genomes (Fig. 1B).

Expression of the zebrafish *abca12* gene during early embryonic development

The temporal expression profile of *abca12* was examined in embryos collected during the first 8 days of development, and the corresponding mRNA levels were determined by reverse transcriptase (RT)-PCR. An undetectable level of expression was noted in embryos at the time of fertilization [0 hours post-fertilization (hpf)], but detectable levels of mRNA transcripts were noted at 6 hpf, with a significant further increase by 1 dpf. During the subsequent days (2-8 dpf), the expression levels remained relatively constant in comparison with the control gene, *β-actin* (Fig. 2A).

Whole-mount in situ hybridization of *abca12* in zebrafish

To determine the spatial expression of *abca12* during different stages of zebrafish development, whole-mount in situ hybridization was performed using probes specific for the *abca12* gene (Fig. 2B). An antisense probe for *abca12* gave specific expression patterns. During the gastrula period, expression of *abca12* was observed in cells of the enveloping layer (EVL; Fig. 2B). Expression of the *abca12* gene in this tissue, which is named periderm after the end of gastrulation, is observed until the end of embryonic development. After 24 hpf, expression of *abca12* was also observed, although at lower levels, in the olfactory vesicle as well as in mucus-secreting cells (Fig. 2B). At the end of embryonic development, expression was observed mainly in olfactory vesicle, pharynx and mucus-secreting cells. A sense probe was used as a control and did not give a specific expression pattern.

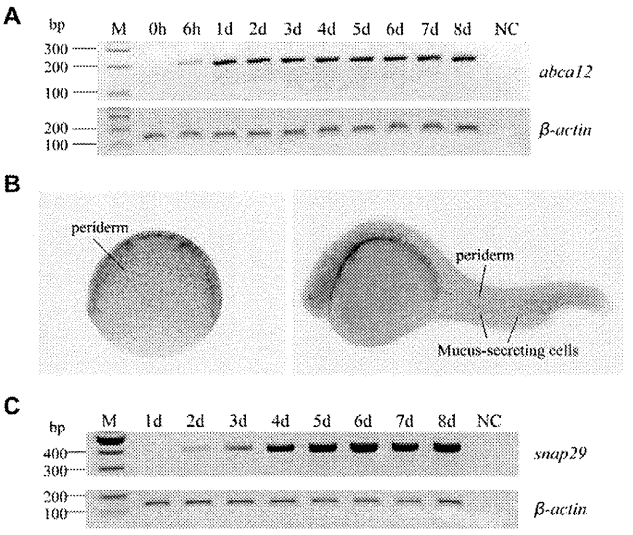

Fig. 2. *abca12* and *snap29* gene expression in normal zebrafish. (A-C) Zebrafish embryos were collected at 0 and 6 hpf and 1-8 dpf, and total RNA was isolated and cDNA prepared. The *abca12* (A) and *snap29* (C) mRNA expression levels were measured by RT-PCR and standardized against the mRNA expression level of the *β-actin* gene. (B) Whole-mount in situ hybridization of embryos at different stages of early development for *abca12* expression; gastrula period (left panel), 24 hpf (right panel).

Morpholino knockdown of *abca12* expression results in an altered skin phenotype

Morpholino antisense oligonucleotide (MO1) directed against a splice donor site in *abca12* was injected into one- to four-cell-stage embryos, and amplification of total RNA was performed by primers corresponding to exons 4 and 5. Using these primers, PCR amplification of *abca12* cDNA resulted in a 189 bp product, whereas amplification of genomic DNA generated a 356 bp product (Fig. 3A). RT-PCR of total RNA extracted from zebrafish 3 days after injection with MO1 revealed that essentially all (>90%) of the pre-mRNA remained unprocessed, attesting to the efficiency of the morpholino knockdown (Fig. 3A). Injection of control morpholinos, either a global standard control MO (scMO) or 5-bp mismatched control (cMO), had no effect on pre-mRNA processing (Fig. 3A).

The effect of the injection of morpholinos into one- to four-cell embryos was first examined by determining the survival of the embryos. Of the 180 embryos injected with *abca12* MO1, 76% survived at 3 dpf, a number that did not statistically differ from the survival of embryos injected with standard control morpholino (81%) (Table 1). At 5 dpf, the survival of embryos injected with MO1 was only 6%, a statistically significant reduction from the survival noted with scMO and uninjected controls (81% and 87%, respectively; $P<0.0001$) (Table 1).

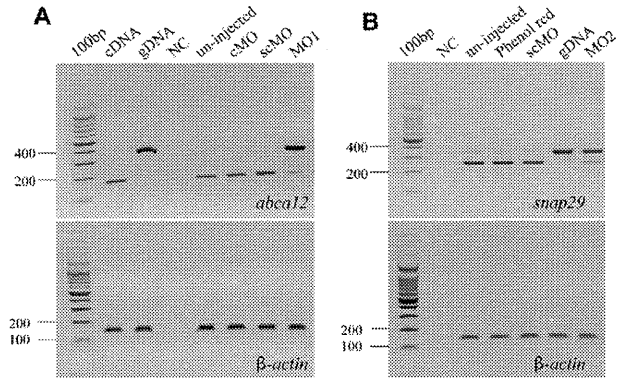

Fig. 3. Knockdown of *abca12* and *snap29* expression by morpholinos. (A) Knockdown of *abca12*. (B) Knockdown of *snap29*. MO1 and MO2 morpholinos (right lanes, the upper panel), which target the splice donor site at the exon-4–intron-4 border of the corresponding genes, prevents pre-mRNA splicing. The consequences of MO1 on *abca12* pre-mRNA splicing and MO2 on *snap29* mRNA splicing were determined by RT-PCR. The results showed the retention of intron 4 in the majority of mRNA transcripts (>90%) as compared with the normally transcribed control. The mRNA levels were normalized by the level of *β-actin* mRNA (lower panels). cDNA and gDNA represent amplification of the corresponding complementary DNA and genomic DNA, respectively. Injections with the 5-bp mismatched control morpholino for *abca12* (cMO) or global standard control morpholino (scMO) did not alter pre-mRNA processing, similar to the uninjected controls or those injected with phenol red.

Examination of the morphology of zebrafish larvae injected with MO1 (n=180) revealed profound changes during development. Although no differences were noted between the morphant and control larvae at 1 dpf, by 3 dpf the morphants had developed noticeable changes in the distribution of pigment along their trunk and tail, in addition to pericardial edema (Fig. 4A). Upon careful examination at 3 dpf, 92% of larvae displayed yolk sac enlargement and severe disruption of their chromatophore distribution, with 75% exhibiting concomitant pericardial edema (Table 1).

Altered epidermal morphology in the morphant larvae

To examine the consequences of the morpholino-mediated knockdown of *abca12* expression in the skin of zebrafish, we first used scanning electron microscopy (SEM) to examine the surface contour and cellular morphology of the epidermis. In 3-dpf controls (n=21), well-demarcated keratinocytes with distinct borders and characteristic microridges were observed (Fig. 5). Examination of the skin surface of the morphant larvae (n=4) revealed perturbations in the architecture of the microridges, with spicules protruding from the center of each keratinocyte. Thus, the development of the top layer of skin during the first 3 days of zebrafish development was perturbed in the absence of Abca12 activity.

Alterations in the epidermis at 3 dpf were further examined by transmission electron microscopy (TEM) both in control and morphant larvae (n=4 in each group). At this developmental stage, normal epidermis consists of two unicellular layers, the superficial layer and the basal layer. The contour of the outer surface of the superficial layer is studded with spicules that correspond to the microridges noted previously on SEM (Fig. 6A). The epidermis rests on a basement membrane, which separates the epidermis from the underlying developing dermis.

The epidermis of the morphant larvae similarly consisted of two cell layers resting on a basement membrane (Fig. 6B). However, in contrast to the control larvae, both layers of the morphant epidermis contained an abundance of electron-dense granules, approximately 440 nm in average diameter. Closer examination of these aggregates at higher magnification suggested the presence of lipid-like vesicles within the larger electron-dense granules (Fig. 6C,D). It should be noted that, although somewhat similar aggregates of electron-dense material were noted in the epidermis of the control specimens, they were localized only to the area of the superficial layer just below the microridges.

Co-injection of human *ABCA12* mRNA rescues the morpholino-mediated phenotype

To test the specificity of the phenotypic changes associated with MO1 injection, a rescue experiment with co-injection of in vitro transcribed human *ABCA12* mRNA was performed. The injection of MO1 alone caused characteristic phenotypic changes, whereas co-injection of human mRNA together with MO1 partially rescued the phenotype (Fig. 4A,B). Specifically, at 5 dpf, the survival of the co-injected larvae was 62%, which is statistically different from the 6% in those injected with MO1 alone (P<0.0001) (Table 1). Also, 27% of co-injected larvae (n=184) had a phenotype that was indistinguishable from the controls. In the remaining 73% of co-injected larvae, the degree of yolk sac enlargement and chromatophore disorganization was noticeably less than in the larvae injected with MO1 alone. Of this 73%, 70% also manifested

Table 1. Survival of and development of phenotype in zebrafish injected with *abca12* morpholino

Experimental group	No. of fish	3 dpf			5 dpf		
		Survival (%)	Skin phenotype (%)	Edema (%)	Survival (%)	Skin phenotype (%)	Edema (%)
Uninjected control	152	87	0	0	87	0	0
scMO	177	81	0	0	81	0	0
abca12 MO1	180	76	92[a]	75[a]	6[a]	0	0
abca12 MO1+ hABCA12 mRNA	184	87[b]	81[b] (milder)	74 (milder)	62[c]	73[c] (milder)	70[c] (milder)

This is a representative experiment in which all groups were followed in parallel. Similar results were obtained in >ten additional experiments with the same design. Skin phenotype refers to epidermal perturbations, disruption of the chromatophore distribution and yolk sac enlargement. Edema is pericardial edema.
scMO, standard control morpholino with no biological function and no target sequence in zebrafish genome (Robu et al., 2007).
[a]Statistical significance between the *abca12* MO1 group and scMO group (Fisher's exact test: P<0.0001).
[b,c]Statistical significance between the *abca12* MO1 group and the *abca12* MO1+hABCA12 mRNA group (Fisher's exact test: [b]P<0.05; [c]P<0.0001).

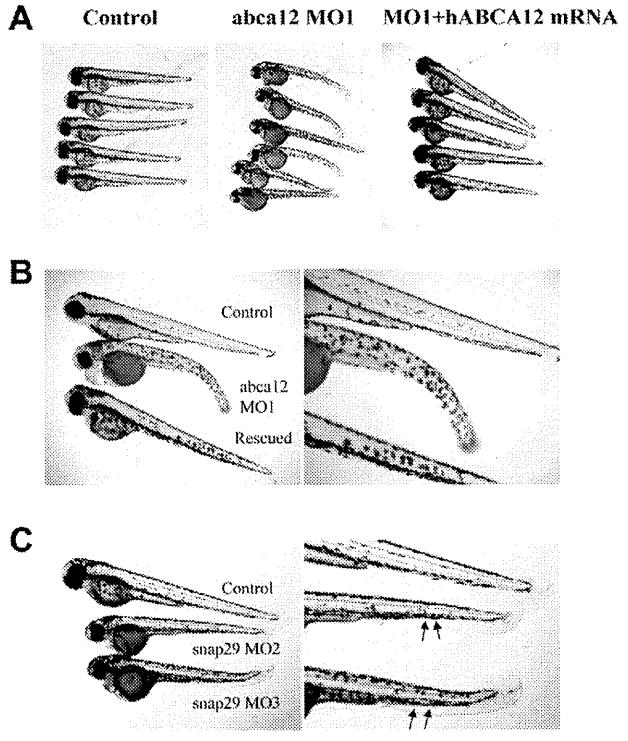

Fig. 4. Zebrafish phenotypes and their mRNA rescue at 3 dpf. (A) Phenotypic appearance of zebrafish larvae after injection with an *abca12* MO1 morpholino (middle panel) compared with control larvae (left panel), and partial rescue with human *ABCA12* mRNA (right panel). (B) Higher magnification of the larvae shown in A. (C) Phenotype of larvae at 3 dpf injected with *snap29* morpholinos MO2 or MO3. The irregular contour of the epidermis is noted by arrows.

pericardial edema. The rescue experiment, in addition to injection of control morpholinos, attested to the specificity of the phenotype documented in the morphant larvae. These experiments also confirmed that the zebrafish *abca12* gene is the functional homolog of human *ABCA12*.

Epidermal perturbations in zebrafish injected with *snap29* morpholino

Because knockdown of *abca12* expression was speculated to interfere with lipid secretion by lamellar granules, resulting in a characteristic epidermal phenotype, we proceeded to test this postulate by interfering with the lipid transport by another, independent mechanism: knockdown of the expression of the *snap29* gene. The corresponding protein, Snap29, has been suggested to mediate lipid transport within the epidermis and the deficiency of SNAP29 expression results in syndromic ichthyosis in patients with CEDNIK syndrome (Rapaport et al., 2010; Sprecher et al., 2005).

Surveying the zebrafish genome database revealed the presence of one *SNAP29*-related gene, *snap29*, on chromosome 8. This gene product had 52% identity with the human gene product at the protein level, and cladogram and syntenic analyses suggested that zebrafish *snap29* is the ortholog of human *SNAP29* (Fig. 1C). The expression of the gene was readily detectable at 2 dpf by RT-PCR and the expression level increased during 3-8 dpf (Fig. 2C). In situ hybridization of larvae showed weak, ubiquitous expression with accentuation of the labeling in the central nervous system marginal zone (not shown).

Injection of a morpholino (MO2) placed on the exon-4–intron-4 junction of the *snap29* gene into one- to four-cell-stage embryos inhibited the processing of pre-mRNA by >90% (Fig. 3B). A second, non-overlapping morpholino (MO3), placed on the intron-4–exon-5 border of the *snap29* gene similarly resulted in >90% inhibition of the splicing of intron 4 (data not shown). Examination of the morphant larvae at 3 dpf (n=165 for MO2, and n=203 for MO3) revealed a phenotype consisting of pigmentary changes, somewhat analogous with those noted with the *abca12* morpholino, in 80% of larvae, and the contour of the epidermis in the tail section was irregular (Fig. 4C). SEM of 20 morphant larvae revealed perturbations in the morphology of the epidermis that were very similar to those noted as a result of *abca12* knockdown (Fig. 5). Examination of the epidermis of the *snap29* morphant larvae (n=4) by TEM at 3 dpf revealed an increase in vesicles, which appeared empty under the same fixation conditions that revealed accumulation of lipid-like material in *abca12* morphant fish (Fig. 6E,F). Thus, interference by morpholino knockdown of the expression of two independent genes, *abca12* and *snap29*, that are involved in lipid transport in the epidermis can lead to similar phenotypic alterations in the epidermal morphology.

DISCUSSION

ABCA12 mutations underlie HI

The molecular basis of HI is linked to mutations in the *ABCA12* gene (Akiyama et al., 2005; Kelsell et al., 2005). Initial approaches utilizing single-nucleotide polymorphism-based chip technology and homozygosity mapping of families with individuals affected with HI placed the candidate gene locus on chromosomal region 2q35, and microsatellite markers narrowed the interval to consist of six genes (Kelsell et al., 2005). Several previous observations pointed to *ABCA12* as a candidate gene within the critical region. First, a characteristic ultrastructural feature of the epidermis in HI is an abnormality in the

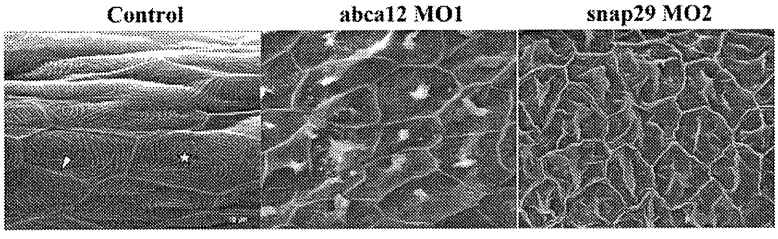

Fig. 5. SEM of the skin surface. The skin of the tail of the control larvae injected with the global standard control morpholino at 3 dpf shows the presence of keratinocytes with well-demarcated cell-cell borders (arrowhead) containing microridges (star; left panel). The morphant larvae injected with MO1 morpholino for *abca12* (middle) or *snap29* (MO2; right panel) revealed perturbed microridge formation with spicules in the center of the keratinocytes.

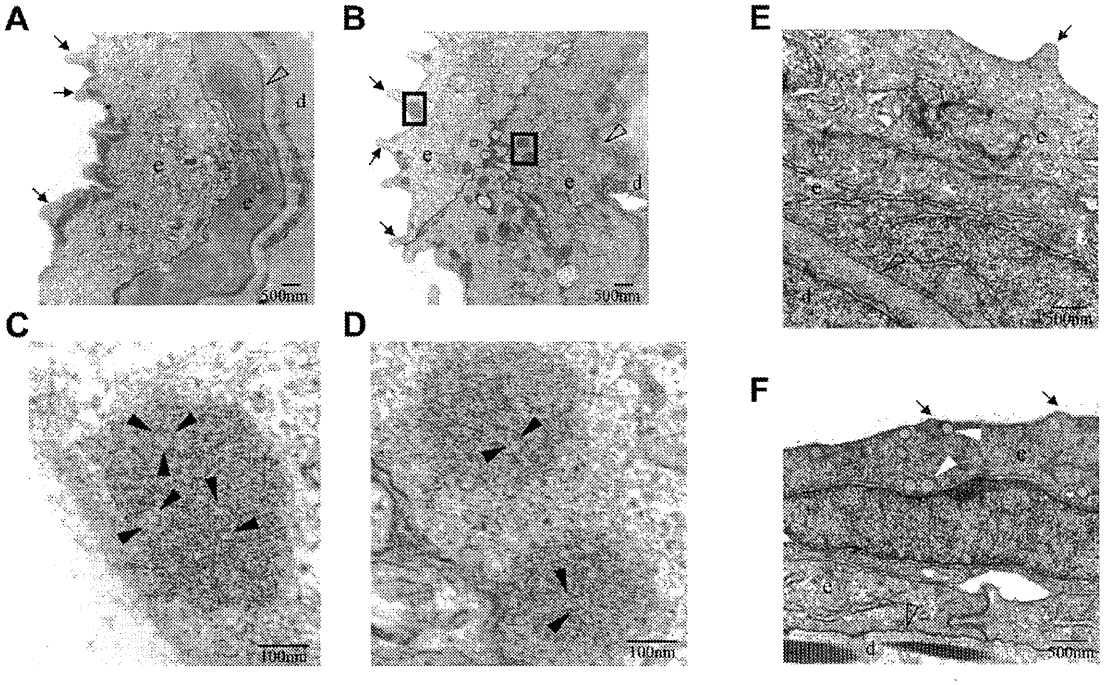

Fig. 6. TEM of 3-dpf larvae injected with *abca12* or *snap29* morpholinos. (A,E) Control morpholino (scMO); (B) *abca12* morpholino (MO1). Boxes surrounding electron-dense subcellular structures in B were examined at higher magnification and are shown in C and D. (F) Injection with *snap29* morpholino (MO2). (A-F) Arrows point to microridges; open arrowheads indicate basement membrane; solid black arrowheads point to the areas of accumulation of putative lipids within the electron-dense granules in C and D; solid white arrowheads in F point to apparently empty vesicles. e, epidermis; d, developing dermis.

localization of epidermal lipids, together with abnormal ultrastructural epidermal lamellar granules (Akiyama, 2006b). *ABCA12* has been suggested to encode a transmembrane transporter protein, which, from sequence homology with several other ABC family members, was thought to be involved in the transport of lipids (Kaminski et al., 2006). Second, the *ABCA12* gene was previously shown to harbor missense mutations in a milder form of ichthyosis, lamellar ichthyosis type 2 (LI2), with some resemblance to the phenotype in patients with HI who survive beyond the immediate postnatal period (Lefèvre et al., 2003). Currently, a total of 53 distinct mutations have been identified in the *ABCA12* gene (Akiyama, 2010).

Expression of *ABCA12* has been localized to lamellar granules. In normal epidermal keratinocytes there is an upregulation of *ABCA12* expression in association with physiological keratinization of the human epidermis (Sakai et al., 2007). Mutations in the *ABCA12* gene result in congested lipid retention in the skin of individuals with HI. It has been suggested that ABCA12 transports ceramides, the major lipid of the stratum corneum of the epidermis. Finally, lamellar-granule-mediated lipid secretion was resumed in the cultured keratinocytes of patients with HI upon transfer of the wild-type *ABCA12* gene (Akiyama et al., 2005). Thus, it is clear that mutations in the *ABCA12* transporter gene underlie HI.

abca12 and zebrafish skin development

In this study, we have demonstrated that zebrafish *abca12* is the ortholog of human *ABCA12*. There is a high degree of conservation of the Walker A and B motifs in addition to the retention of the four transmembrane domains containing one, five, one and five transmembrane segments, respectively. Zebrafish NBF1 and NBF2 domains in the Abca12 protein have 74% and 68% similarity with human NBF1 and NBF2 domains, respectively, at the amino acid level.

Whole-mount in situ hybridization in developing zebrafish embryos revealed that *abca12* was expressed in the EVL and the periderm. The EVL first appears at the 64-cell stage of development (~2 hpf) and is the outermost monolayer of cells surrounding the embryo. The EVL eventually gives rise to the periderm, which is thought to ultimately be replaced by the superficial stratum of the epidermis (Kimmel et al., 1995; Le Guellec et al., 2004). Although the physiology of zebrafish skin is still largely unexplored, the fact that *abca12* is expressed in the skin suggests its importance in normal skin development. This hypothesis is further strengthened by the results from our morpholino experiments. Injecting a morpholino that inhibited pre-mRNA splicing by >90% produced alterations in chromatophore distribution and the abnormal retention of lipids in both layers of the epidermis. Not only does this suggest that *abca12* is responsible for lipid transport in zebrafish, but the abnormal accumulation of lipids throughout the epidermis is a frequent finding in individuals with HI. Finally, the rescue of this phenotype by co-injection of human *ABCA12* mRNA shows that the phenotype is the result of *abca12* knockdown and not due to an off-target effect. In this context, it should be emphasized that the EVL-derived skin in zebrafish is embryologically different from the mammalian skin. Specifically, zebrafish epidermis does not undergo terminal differentiation, which in human skin culminates in the development of stratum corneum with barrier function. Emphasizing this

difference is the fact that survey of the current zebrafish genome database (Ensembl, Zebrafish Zv9; http://www.ensembl.org/Danio_rerio/Info/Index) does not reveal the presence of filaggrin, involucrin and trichohyalin genes, which are crucial for development of the stratum corneum in human epidermis (Li et al., 2011).

The role of lipids in epidermal development is further emphasized by our findings that knockdown of the expression of an independent gene, *snap29*, results in a similar epidermal phenotype as noted in *abca12* mutant larvae. Snap29 has been postulated to mediate lipid transport in the epidermis by facilitating membrane fusion of lamellar granules (Sprecher et al., 2005). Thus, interference of lipid trafficking by knockdown of two independent genes results in phenocopies of the epidermal perturbations in zebrafish, mimicking epidermal alterations in different forms of ichthyosis. It should be noted that, similar to the CEDNIK syndrome, ichthyosis has been reported in association with mental retardation, enteropathy, deafness, peripheral neuropathy and keratodermia, dubbed as the MEDNIK syndrome (Montpetit et al., 2008). This constellation was shown to be associated with a homozygous splice-site mutation in the *AP1S1* gene, encoding a subunit of the adaptor protein complex that regulates clathrin-coated vesicle assembly, protein cargo sorting, and vesicular trafficking between organelles in eukaryotic cells (Montpetit et al., 2008). The pathogenic effect of this mutation was validated by knockdown of *ap1s1* expression in zebrafish by a morpholino, resulting in perturbation in skin formation, reduced pigmentation and motility deficits. These findings, together with our observations in *snap29* mutant larvae, attest to the importance of vesicular trafficking in epidermal morphogenesis.

As indicated by morphological observations of the developing epidermis in zebrafish in comparison with human skin, there are clear differences. For example, the embryological origin of the EVL (periderm) in zebrafish is distinct from the basal layer in embryonic skin. In spite of this difference, there is an increasing body of evidence suggesting that the underlying molecular differentiation pathways are conserved between mammals and the zebrafish epidermis, based on molecular homologies (Sabel et al., 2009; Slanchev et al., 2009). Our work highlighting the early *abca12* expression in the EVL seems to support the conclusions that EVL forms the external layer of the embryonic and larval dermis and represents the initial differentiation of a true epidermis (Fukazawa et al., 2010).

Collectively, our results highlight the role of lipid transport and vesicular trafficking in epidermal development, and the results further suggest that zebrafish can serve as a model system to study different variants of ichthyosis, such as HI and the CEDNIK syndrome. Besides increasing our understanding of the disease mechanisms involved in ichthyotic syndromes, this model system is potentially useful for testing novel treatment modalities, for example by performing a small molecule library screen for compounds that are able to suppress the phenotype.

METHODS

Maintenance of zebrafish

Adult wild-type zebrafish were maintained under standard conditions at 28.5°C. Zebrafish embryos and larvae were also maintained at 28.5°C in a special embryo medium. All animals were housed in the zebrafish facility at Thomas Jefferson University and were cared for and used in accordance with University Institutional Animal Care and Use Committee guidelines and permission.

Phylogenetic and syntenic analyses

The genomic sequences of zebrafish were extracted from the Ensembl database. The zebrafish protein sequences were aligned with the corresponding proteins in different species by using ClustalW software (http://www.ebi.ac.uk/clustalw/).

The accession numbers for the *abca12* gene products in different species are: *E. caballus* (ENSECAP00000007797), *C. lupus familiaris* (XP_536058), *B. taurus* (XP_001788086), *H. sapiens* (NP_775099), *P. troglodytes* (XP_516070), *M. musculus* (XP_001002308), *R. norvegicus* (XP_237242), *G. gallus* (XP_421867), *D. rerio* (XP_686632) and *O. latipes* (ENSORLP00000020129). The accession numbers for *ABCC10* in *H. sapiens* is NP_258261. The accession numbers for *Abcc6* in different species are: *M. musculus* (NP_061265), *H. sapiens* (NP_001162), *D. rerio* (ENSDARP00000065432), *T. nigroviridis* (ENSTNIP00000015029) and *T. rubripes* (ENSTRUP00000029065).

The accession numbers for the *snap29* gene products in different species are: *H. sapiens* (NP_004773.1), *P. troglodytes* (XP_514997.2), *M. mulatta* (XP_001086227.1), *M. musculus* (NP_075837.3), *R. norvegicus* (NP_446262.3), *C. familiaris* (XP_543568.2), *B. taurus* (NP_001069427.1), *G. gallus* (NP_001025823.1), *D. rerio* (XP_700124.3), *S. salar* (NP_001134759.1), *X. laevis* (NP_001080076.1) and *A. thaliana* (NP_196405.1).

Phylogenetic analyses were conducted in the Molecular Evolution Genetics Analysis software (MEGA) version 4.0 (Tamura et al., 2007). The cladogram was constructed using the Neighbor-Joining method (Saitou and Nei, 1987). The Kimura two-parameter method was used to compute the evolutionary distances (Zuckerkandl and Pauling, 1965). The statistical reliance of NJ tree branches was evaluated using 1000 bootstrap samples.

For syntenic analysis, the orientation and chromosomal positions of *abca12* and *snap29* and their adjacent genes were determined manually from the gene orientations in the current Ensembl database. The zebrafish (Zv9), human (GRCh37/hg19), mouse (NCB137/mm9) and chicken (WUGSC2.1/galGal3) genome assembly versions were used for this analysis.

In situ hybridization

Whole-mount in situ hybridization was performed as described previously (Thisse and Thisse, 2008). Collected zebrafish embryos were fixed in 4% paraformaldehyde before hybridization. Digoxigenin (DIG)-labeled antisense and sense probes were synthesized. After hybridization, detection was performed with an anti-DIG antibody coupled to alkaline phosphatase.

Morpholinos and microinjection

Morpholino oligonucleotides were obtained from Gene Tools, LLC (Corvalis, OR). The morpholino oligomer sequences were written from 5′ to 3′, to correspond to the following genomic sequences (brackets surround the morpholino target sequence, exon sequences are capitalized, intron sequences are in lowercase, and nucleotide substitutions are bolded). For *abca12* knockdown: splice donor site morpholino (MO1), tgggaaataaatgtaatttacctgt, targets the exon-4–intron-4 junction, AAATGAAATAACTGA[ACAGgta-aattacatttatttccca]acggtc; 5-base pair mismatched control morpholino for *abca12* (cMO): tgg**c**aaa**a**aaat**c**taatttac**g**t**c**t. For *snap29* knockdown: splice donor site morpholino (MO2), ctgctcttgtgtttctcacccaggt, targets the exon-4–intron-4 junction,

GACAGAA[ACCTGGgtgagaaacacaagacag]cttctctcata; a second *snap29* splice junction morpholino (MO3) targets the intron 4-exon 5 border, ctcatctggaggacacaaacacaca, agtgtgtgtg[tgtgtg-tttgtgtcctccagATGAG]ATGTCTCTGGGTC. Global standard control morpholino (scMO), cctcttacctcagttacaatttata, has no target sequence in the zebrafish genome and is, therefore, inactive.

Embryos at the one- to four-cell stage were injected with an *abca12* morpholino (MO1, 25.6 ng) or *snap29* morpholinos (MO2, 2.6 ng and MO3, 5.2 ng) using glass microelectrodes fitted to a gas pressure injector (PL1-100, Harvard Apparatus). Electrodes were pulled (P-97, Flaming/Brown) and filled with morpholino and phenol red (final concentration 0.025%) to visualize the injected embryos. The embryos were then followed for viability, morphology and mRNA expression levels.

Total RNA isolation and cDNA synthesis

Zebrafish embryos were collected at 0 as well as 6 hpf and 1-8 dpf. They were disintegrated by pipetting through a 21 gauge needle and total RNA was extracted using TRIzol reagent (Invitrogen, Carlsbad, CA). To remove contaminating genomic DNA, RNase-free DNase I digestion (Fisher Scientific, St Louis, MO) was performed. 1 μg of total RNA was reverse transcribed using the Superscript III First-Strand cDNA synthesis kit (Invitrogen) according to the manufacturer's protocol. Controls were performed by omitting the reverse transcriptase enzyme. All cDNA samples were stored at −20°C for future use.

PCR amplification of cDNA

abca12 cDNA was amplified by PCR using a forward primer on exon 4 (5′-ATCTGGGACAACTTGGGCAACT-3′), and a reverse primer on exon 5 (5′-TCATCTGGTCAGCAGTTCCAGAGA-3′). The *snap29* cDNA was amplified using a forward primer on exon 4 (5′-TTCTGCTGCTCTTGATAACGGCT-3′), and a reverse primer on exon 5 (5′-TTTAAGGCTTTTGAGCTGCCGGTT-3′). Primers for the zebrafish *β-actin* gene (fwd: 5′-ATCTGGCACCACACCTTCTACAATG; rev: 5′-GGGGTG-TTGAAGGTCTCAAACATGAT) were used as a positive control. PCR was performed using Taq polymerase and Q buffer (Qiagen, Valencia, CA), according to the manufacturer's instructions. The PCR conditions were as follows: an initial denaturation at 94°C for 5 minutes, followed by 35 cycles of 94°C for 1 minute; 58°C for 1 minute; 72°C for 1 minute; and finally 72°C for 10 minutes. The intensity of the bands was quantified using ImageQuant version 5.0 software (Molecular Dynamics, Sunnyvale, CA).

mRNA rescue experiments

Capped full-length human mRNA corresponding to *ABCA12* was transcribed from an expression vector pCMV-Tag4B using the T3 mMessage mMachine kit (Ambion, Austin, TX). The morpholino was injected into one- to four-cell-stage embryos either alone or in combination with mRNA (2.3 ng) and followed for viability and morphology.

Scanning electron microscopy

Samples were fixed in neutral buffered formalin at room temperature for 2 hours, followed by a rinse with phosphate buffered saline and an ethanol dehydration series of exchanges by completely replacing each successively higher ethanol solution with the next higher (20, 30, 50, 75, 95 and 100%). Samples were then incubated for 15 minutes in a 1.5 ml micro test tube containing 1,1,2-Trichloro-1,2,2-trifluoroethane before covering the open micro test tube with parafilm, punching holes in it with a 30G needle, and situating it under a fume hood where it was dried by turbulent air flow. Samples were then mounted onto stubs with carbon paint and coated in 50 nm of gold using a sputter coater. Specimens were imaged in a JEOL-T330A scanning electron microscope (JEOL, Tokyo, Japan) at 15 kV.

TRANSLATIONAL IMPACT

Clinical issue

Ichthyosis comprises a group of cutaneous disorders characterized by dry, scaly skin and a broad spectrum of other phenotypic manifestations. One of the most severe forms of ichthyosis is known as harlequin ichthyosis (HI); neonates affected with HI are born encased in a thick skin that restricts their movement and frequently die shortly after birth. Some forms of ichthyosis are syndromic; for example, CEDNIK syndrome is so-named because it consists of cerebral dysgenesis, neuropathy, ichthyosis and keratoderma. Details of the pathomechanisms of HI have recently been revealed through molecular genetics, which showed that patients with this disorder carry mutations in the *ABCA12* gene. Examination of *Abca12*$^{-/-}$ mice suggested that this gene encodes a transmembrane transporter present in the epidermis that is postulated to transport lipids (specifically ceramides) and that is required for formation of the stratum corneum on the surface of the skin. Although the mouse model is useful in that it recapitulates features of human HI, drawbacks include the long gestational period and the small number of offspring produced per litter. CEDNIK syndrome is caused by mutations in the *SNAP29* gene, which is required for normal vesicle trafficking and lipid transport in the epidermis. There is no animal model for this syndrome.

Results

To create alternative, more expedient model systems to investigate pathological mechanisms of both HI and CEDNIK syndrome, the authors of this study knocked down the homologs of *ABCA12* and *SNAP29* in zebrafish embryos (*Danio rerio*). Morpholino antisense oligonucleotides targeted to exon-intron splice junctions were used to inhibit the splicing of *abca12* or *snap29* pre-mRNA. Inhibition of processing of either one of these mRNAs was accompanied by changes in the distribution of pigment along the trunk and tail of the fish as early as 2 days post-fertilization (dpf). Examination of epidermal morphology by scanning electron microscopy revealed perturbations in the surface contour of the keratinocytes, with loss of characteristic microridges and development of pathological spicules protruding from the center of each keratinocyte. These epidermal changes were accompanied by premature demise of the fish by 5 dpf. Transmission electron microscopy revealed an abundance of electron-dense granules in both morphants: lipid-like vesicles were seen in *abca12* knockdown fish, whereas the epidermis of *snap29* knockdown animals showed the presence of apparently empty vesicles.

Implications and future directions

This study demonstrates that inhibition of *abca12* or *snap29* gene splicing in zebrafish leads to epidermal perturbations that are similar to those seen in human patients with various forms of ichthyosis. In addition, it suggests that interfering with two independent pathways involved in lipid transport can result in phenotypically similar perturbations in epidermal morphogenesis. These systems can serve as models to study ichthyosis, and provide a means to develop pharmacological approaches towards treatment of this currently intractable group of diseases. Finally, in a broader sense, this study attests to the feasibility of using zebrafish as a model system to study heritable skin diseases.

Transmission electron microscopy

Samples were collected and fixed overnight at 4°C in 2.5% gluteraldehyde, 2% paraformaldehyde and 0.1 M sodium cacodylate. Samples were then washed in 0.1 M sodium cacodylate before undergoing secondary fixation in 2% osmium tetroxide, 1.5% potassium ferricyanide and 0.1 M sodium. Samples were again washed with 0.1 M sodium cacodylate followed by deionized water before undergoing en block staining with 2% uranyl acetate. Samples were washed again with deionized water, then dehydrated in a graded ethanol series and embedded in EMbed-812 (EMS, Hatfield, PA). Ultrathin sections (60 nm) were cut and analyzed using a JEOL JEM-1010 transmission electron microscope fitted with a Hamamatsu digital camera (Hamamatsu Photonics, Hamamatsu City, Japan) and AMT Advantage image capture software (AMT, Danvers, MA).

Statistical analysis

Risk differences and 95% confidence intervals were calculated between experimental groups with regards to survival, skin phenotype and edema in Table 1, for 3 dpf and 5 dpf separately. Fisher's exact test was used to determine the difference between proportions because of the presence of cells with zero observations. Adjustments for multiple comparisons were performed using False Discovery Rate, and it is these adjusted *P*-values that are reported. Analyses were conducted using SAS 9.2 (SAS Institute, Cary, NC).

ACKNOWLEDGEMENTS

The authors thank the following colleagues for advice and assistance: Wolfgang Driever, Institute for Biology I, University of Freiburg; Raymond Meade, Biomedical Imaging Core Facility, University of Pennsylvania; Gerald Harrison, Department of Biochemistry, School of Dental Medicine, University of Pennsylvania; Jean-Yves Sire, Equipe "Evolution et Développement du Squelette", Université Paris; Eijiro Adachi, Department of Matrix Biology and Tissue Regeneration, Graduate School of Medical Sciences, Kitasato University; Ulrich Rodeck, Gabor Kari, April Aguillard, Adele Donahue and Andrzej Fertala, Department of Dermatology and Cutaneous Biology, Thomas Jefferson University; Terry Hyslop and Jocelyn Andrel, Department of Pharmacology and Experimental Therapeutics, Thomas Jefferson University. Carol Kelly assisted in manuscript preparation. This study was supported by the NIH/NIAMS grant R01AR055225 to J.U.; by the University of Virginia to C.T. and B.T. Q.L. is a recipient of a Research Career Development Award from the Dermatology Foundation.

COMPETING INTERESTS

The authors declare that they do not have any competing or financial interests.

AUTHOR CONTRIBUTIONS

Q.L., M.F., C.T. and B.T. performed the experiments; M.A. provided reagents; H.S. and E.S. interpreted the data and edited the manuscript; S.-Y.H. contributed to the data analysis; J.U. developed the concept, interpreted the data and prepared the manuscript.

REFERENCES

Akiyama, M. (2006a). Harlequin ichthyosis and other autosomal recessive congenital ichthyoses: the underlying genetic defects and pathomechanisms. *J. Dermatol. Sci.* **42**, 83-89.

Akiyama, M. (2006b). Pathomechanisms of harlequin ichthyosis and ABCA transporters in human diseases. *Arch. Dermatol.* **142**, 914-918.

Akiyama, M. (2010). *ABCA12* mutations in harlequin ichthyosis, congenital ichthyosiform erythroderma and lamellar ichthyosis. *Hum. Mutat.* **31**, 1090-1096.

Akiyama, M., Sugiyama-Nakagiri, Y., Sakai, K., McMillan, J. R., Goto, M., Arita, K., Tsuji-Abe, Y., Tabata, N., Matsuoka, K. and Sasaki, R. (2005). Mutations in lipid transporter ABCA12 in harlequin ichthyosis and functional recovery by corrective gene transfer. *J. Clin. Invest.* **115**, 1777-1784.

Brown, S. J. and Irvine, A. D. (2008). Atopic eczema and the filaggrin story. *Semin. Cutan. Med. Surg.* **27**, 128-137.

Brown, S. J. and McLean, W. H. I. (2008). Eczema genetics: current state of knowledge and future goals. *J. Invest. Dermatol.* **129**, 543-552.

Elias, P. M., Crumrine, D., Rassner, U., Hachem, J. P., Menon, G. K., Man, W., Choy, M. H., Leypoldt, L., Feingold, K. R. and Williams, M. L. (2004). Basis for abnormal desquamation and permeability barrier dysfunction in RXLI. *J. Invest. Dermatol.* **122**, 314-319.

Fuchs-Telem, D., Stewart, H., Rapaport, D., Nousbeck, J., Gat, A., Gini, M., Lugassy, Y., Emmert, S., Eckl, K., Hennies, H. C. et al. (2011). CEDNIK syndrome results from loss-of-function mutations in SNAP29. *Br. J. Dermatol.* **164**, 610-616.

Fukazawa, C., Santiago, C., Park, K. M., Deery, W. J., Gomez de la Torre Canny, S., Holterhoff, C. K. and Wagner, D. A. (2010). poly/chuk/ikk1 is required for differentiation of the zebrafish embryonic epidermis. *Dev. Biol.* **346**, 272-283.

Kaminski, W. E., Piehler, A. and Wenzel, J. J. (2006). ABC A-subfamily transporters: structure, function and disease. *Biochim. Biophys. Acta* **1762**, 510-524.

Kari, G., Rodeck, U. and Dicker, A. P. (2007). Zebrafish: an emerging model system for human disease and drug discovery. *Clin. Pharmacol. Ther.* **82**, 70-80.

Kelsell, D. P., Norgett, E. E., Unsworth, H., Teh, M. T., Cullup, T., Mein, C. A., Dopping-Hepenstal, P. J., Dale, B. A., Tadini, G. and Fleckman, P. (2005). Mutations in ABCA12 underlie the severe congenital skin diseases harlequin ichthyosis. *Am. J. Hum. Genet.* **76**, 794-803.

Kimmel, C. B., Ballard, W. W., Kimmel, S. R., Ullmann, B. and Schilling, T. F. (1995). Stages of embryonic development of the zebrafish. *Dev. Dyn.* **203**, 253-310.

Le Guellec, D., Morvan-Dubois, G. and Sire, J. Y. (2004). Skin development in bony fish with particular emphasis on collagen deposition in the dermis of the zebrafish (Danio rerio). *Int. J. Dev. Biol.* **48**, 217-232.

Lefèvre, C., Audebert, S., Jobard, F., Bouadjar, B., Lakhdar, H., Boughdene-Stambouli, O., Blanchet-Bardon, C., Heilig, R., Foglio, M. and Weissenbach, J. (2003). Mutations in the transporter ABCA12 are associated with lamellar ichthyosis type 2. *Hum. Mol. Genet.* **12**, 2369-2378.

Li, Q., Frank, M., Thisse, C., Thisse, B. and Uitto, J. (2011). Zebrafish: a model system to study heritable skin diseases. *J. Invest. Dermatol.* **131**, 565-571.

McGrath, J. A. and Uitto, J. (2008). The filaggrin story: novel insights into skin-barrier function and disease. *Trends Mol. Med.* **14**, 20-27.

Montpetit, A., Côté, S., Brustein, E., Drouin, C. A., Lapointe, L., Boudreau, M., Meloche, C., Drouin, R., Hudson, T. J., Drapeau, P. et al. (2008). Disruption of AP1S1, causing a novel neurocutaneous syndrome, perturbs development of the skin and spinal cord. *PloS Genet.* **4**, e1000296.

Rapaport, D., Lugassy, Y., Sprecher, E. and Horowitz, M. (2010). Loss of SNAP29 impairs endocytic recycling and cell motility. *PloS ONE* **5**, e9759.

Sabel, J. L., d'Alençon, C., O'Brien, E. K., Van Otterloo, E., Lutz, K., Cuykendall, T. N., Schutte, B. C., Houston, D. W. and Cornell, R. A. (2009). Maternal interferon regulatory factor 6 is required for the differentiation of primary superficial epithelia in Danio and Xenopus embryos. *Dev. Biol.* **325**, 249-263.

Saitou, N. and Nei, M. (1987). The neighbor-joining method: a new method for reconstructing phylogenetic trees. *Mol. Biol. Evol.* **4**, 406-425.

Sakai, K., Akiyama, M., Sugiyama-Nakagiri, Y., McMillan, J. R., Sawamura, D. and Shimizu, H. (2007). Localization of ABCA12 from golgi apparatus to lamellar granules in human upper epidermal keratinocytes. *Exp. Dermatol.* **16**, 920-926.

Slanchev, K., Carney, T. J., Stemmler, M. P., Koschorz, B., Amsterdam, A., Schwarz, H. and Hammerschmidt, M. (2009). The epithelial cell adhesion molecule EpCAM is required for epithelial morphogenesis and integrity during zebrafish epiboly and skin development. *PLoS Genet.* **5**, e1000563.

Smyth, I., Hacking, D. F., Hilton, A. A., Mukhamedova, N., Meikle, P. J., Ellis, S., Satterley, K., Collinge, J. E., de Graaf, C. A. and Bahlo, M. (2008). A mouse model of harlequin ichthyosis delineates a key role for Abca12 in lipid homeostasis. *PLoS Genet.* **4**, e1000192.

Sprecher, E., Ishida-Yamamoto, A., Mizrahi-Koren, M., Rapaport, D., Goldsher, D., Indelman, M., Topaz, O., Chefetz, I., Keren, H., O'Brien, T. J. et al. (2005). A mutation in SNAP29, coding for a SNARE protein involved in intracellular trafficking, causes a novel neurocutaneous syndrome characterized by cerebral dysgenesis, neuropathy, ichthyosis, and palmoplantar keratoderma. *Am. J. Hum. Genet.* **77**, 242-251.

Sundberg, J. P., Boggess, D., Hogan, M. E., Sundberg, B. A., Rourk, M. H., Harris, B., Johnson, K., Dunstan, R. W. and Davisson, M. T. (1997). Harlequin ichthyosis (ichq): a juvenile lethal mouse mutation with ichthyosiform dermatitis. *Am. J. Pathol.* **151**, 293-310.

Tamura, K., Dudley, J., Nei, M. and Kumar, S. (2007). MEGA4: molecular evolutionary genetics analysis (MEGA) software version 4.0. *Mol. Biol. Evol.* **24**, 1596-1599.

Thisse, C. and Thisse, B. (2008). High resolution in situ hybridization on whole-mount zebrafish embryo. *Nat. Protoc.* **3**, 59-69.

Tusnády, G. E., Sarkadi, B., Simon, I. and Váradi, A. (2006). Membrane topology of human ABC proteins. *FEBS Lett.* **580**, 1017-1022.

Yanagi, T., Akiyama, M., Nishihara, H., Sakai, K., Nishie, W., Tanaka, S. and Shimizu, H. (2008). Harlequin ichthyosis model mouse reveals alveolar collapse and severe fetal skin barrier defects. *Hum. Mol. Genet.* **17**, 3075-3083.

Zuckerkandl, E. and Pauling, L. (1965). Evolutionary divergence and convergence in proteins. In *Evolving Genes and Proteins* (ed. V. Bryson and H. J. Vogel), pp. 97-166. New York: Academic Press.

for allergen, *S. aureus* colonization, skin barrier dysfunction and AD deterioration is recently reported [8]. The virulence factors produced by *S. aureus* have various biological characteristics to destroy epithelial barrier, inhibit opsonization, interfere neutrophil chemotaxis, inactivate neutrophil cytolysis and antimicrobial peptide [4,9,10]. Although further studies are required to examine this hypothesis, current evidence is sufficient to conclude that *S. aureus* and possibly some other skin microflora are directly related to aggravation of healthy skin conditions. Similar to diseased skin, *S. aureus* and subtle dysfunction of skin barrier in healthy skin can also be caught in a vicious circle, resulting in further breakdown of skin barrier and progress to outright deterioration.

These findings are meaningful as a first study to demonstrate that *S. aureus* is involved in skin deterioration, even in apparently healthy skin.

References

[1] Meulemans L, Hermans K, Duchateau L, Haesebrouck F. High and low virulence *Staphylococcus aureus* strains in a rabbit skin infection model. Vet Microbiol 2007;125:333–40.
[2] Lowy FD. *Staphylococcus aureus* infections. N Engl J Med 1998;339:520–32.
[3] Leyden JJ, McGinley KJ, Nordstrom KM, Webster GF. Skin microflora. J Invest Dermatol 1987;88::65s–72s.
[4] Iwatsuki K, Yamasaki O, Morizane S, Oono T. Staphylococcal cutaneous infections: invasion, evasion and aggression. J Dermatol Sci 2006;42:203–14.
[5] Katsuyama M, Ichikawa H, Ogawa S, Ikezawa Z. A novel method to control the balance of skin microflora. Part 1. Attack on biofilm of *Staphylococcus aureus* without antibiotics. J Dermatol Sci 2005;38:197–205.
[6] Williams RE, Gibson AG, Aitchison TC, Lever R, Mackie RM. Assessment of a contact-plate sampling technique and subsequent quantitative bacterial studies in atopic dermatitis. Br J Dermatol 1990;123:493–501.
[7] Chikakane K, Takahashi H. Measurement of skin pH and its significance in cutaneous diseases. Clin Dermatol 1995;13:299–306.
[8] Hirasawa Y, Takai T, Nakamura T, Mitsuishi K, Gunawan H, Suto H, et al. *Staphylococcus aureus* extracellular protease causes epidermal barrier dysfunction. J Invest Dermatol 2010;130:614–7.
[9] Clarke SR, Mohamed R, Bian L, Routh AF, Kokai-Kun JF, Mond JJ, et al. The *Staphylococcus aureus* surface protein IsdA mediates resistance to innate defenses of human skin. Cell Host Microb 2007;1:199–212.
[10] Mack D, Becker P, Chatterjee I, Dobinsky S, Knobloch J, Peters G, et al. Mechanisms of biofilm formation in *Staphylococcus epidermidis* and *Staphylococcus aureus*: functional molecules, regulatory circuits, and adaptive responses. Int J Med Microbiol 2004;294:203–12.

Kyeho Shin[a,b]
[a]*Skin Research Institute, R&D Center, AmorePacific Corporation, Yongin-si, Gyeonggi-do, Republic of Korea*
[b]*Biomaterials Process Engineering Lab, Department of Biotechnology, Yonsei University, Seoul, Republic of Korea*

Tae Ryong Lee
Enyoung Lee
Yoon Hyeok Jeong
Yuna Yun
Tae Hun Park
Hankon Kim
Skin Research Institute, R&D Center, AmorePacific Corporation, Yongin-si, Gyeonggi-do, Republic of Korea
Kashif Ghafoor

Jiyong Park*
Biomaterials Process Engineering Lab, Department of Biotechnology, Yonsei University, Seoul, Republic of Korea
*Corresponding author. Tel.: +82 2 2123 2888; fax: +82 2 362 7265
E-mail address: foodpro@yonsei.ac.kr (J. Park)

25 October 2010
15 April 2011
8 May 2011
doi:10.1016/j.jdermsci.2011.05.003

Letter to the Editor

LEDGF/DFS70 activates the MK2/IL6/STAT3 pathway in HaCaT

Lens epithelium-derived growth factor (LEDGF), also known as dense fine speckles 70 kDa protein (DFS70), was isolated as a transcription cofactor, a survival factor and a target of autoantibodies in atopic dermatitis [1–3]. LEDGF/DFS70 has been implicated as a key player in cancer [4]. Psoriasis is a common skin disorder that is characterized by abnormal differentiation of the epidermal keratinocytes (KCs), inflammatory cells recruitment and changes in the endothelial vascular system. It has been suggested that psoriatic KCs have abnormal expression of various cytokines and chemokines, and deregulation of several signaling pathways. For example, psoriatic KCs are characterized by activation of the signal transducer and activator of transcription 3 (STAT3) [5]. Activated TNF-α and MAPK-activated protein kinase 2 (MK2) have also been observed in lesional psoriatic epidermis [6].

We recently found that LEDGF/DFS70 localizes to the nuclei of spinous layers as well as the basal layer of psoriatic skin, although LEDGF/DFS70 is restricted to the cytoplasm in cells of normal spinous layers [7,8]. We also generated stable cell lines which constitutively express enhanced green fluorescent protein-tagged LEDGF (EGFP-LEDGF-HaCaT) or EGFP alone (EGFP-HaCaT) as a control, and we demonstrated that LEDGF/DFS70 regulated the IL-6 via p38 phosphorylation and deregulated S100A7, S100A9 and filaggrin. In light of this, it was suggested that LEDGF/DFS70 plays a pivotal role in activating psoriatic KCs. This study aims to clarify how LEDGF/DFS70 contributes to the formation of psoriatic skin lesions.

To determine whether minichromosome maintenance 2 (MCM2) phosphorylation is increased in EGFP-LEDGF-HaCaT, we performed Western blot analyses. As shown in Fig. 1a, MCM2 (Ser53) was more phosphorylated in EGFP-LEDGF-HaCaT than in EGFP-HaCaT, although the levels of total MCM2 and MCM2 phosphorylation (Ser40/41) were the same. LEDGF/DFS70 has been shown to interact with the Cdc7-activator of S-phase kinase (ASK), which is essential for initiation of DNA replication throughout the S-phase, and LEDGF/DFS70 has been demonstrated to stimulate its enzymatic activity, increasing phosphorylation of MCM2 (Ser53) *in vitro* [9]. Our results are compatible with the previous reports and suggest that LEDGF/DFS70 may function as an S-phase regulator in the nuclei of proliferating KCs. To determine whether the Cdc7 is involved in MCM2 phosphorylation (Ser53) in EGFP-LEDGF-HaCaT, small interfering RNA (siRNA) was used to reduce Cdc7 expression (siCdc7) in EGFP-LEDGF-HaCaT, and then the amount of phosphorylated MCM2 (Ser53) was measured. Fig. 1b shows that the phosphorylation level of MCM2 (Ser53) was reduced compared to the controls (siCD4) when the Cdc7 protein level was reduced by siRNA.

We previously reported that EGFP-LEDGF-HaCaT have higher IL-6 expression and higher phosphorylation of STAT3 than EGFP-HaCaT has [7]. The gp130 receptor constitutes an essential signal transducing component of the IL-6 receptor complex, and IL-6-

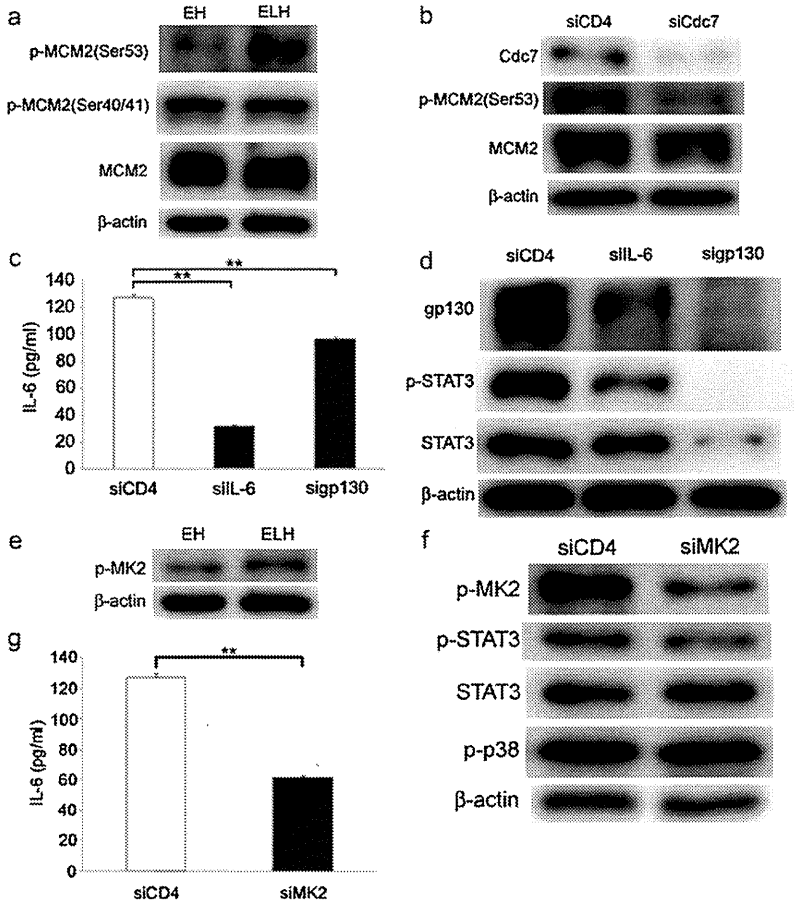

Fig. 1. MCM2 and MK2 are activated in EGFP-LEDGF-HaCaT (a, e); Western blot of lysates from EGFP-LEDGF-HaCaT transfected with several specific small interfering RNAs (b–d, f, g). (a, e) Lysates of EGFP-LEDGF-HaCaT (ELH) and EGFP-HaCaT (EH) incubated for 72 h and analyzed by Western blot for MCM2, phosphorylated MCM2 (p-MCM2), phosphorylated MK2 (p-MK2) and β-actin. (b–d, f, g) EGFP-LEDGF-HaCaT transfected with small interfering (si) RNA against Cdc7 (siCdc7), IL-6 (siIL-6), gp130 (sigp130), MK2 (siMK2) and CD4 (siCD4). After 72 h incubation of the cells, proteins of Cdc7, MCM2, p-MCM2, IL-6, gp130, STAT3, phosphorylated STAT3 (p-STAT3), p-MK2, phosphorylated p38 (p-p38) and β-actin were evaluated by ELISA or Western blot analysis. Statistical significance between groups was assessed by paired Student's *t*-test ($n = 4$). Error bars represent the SEM. $^{**}P < 0.01$.

induced tyrosine phosphorylation of gp130 leads to the activation of STAT3. To determine whether increased IL-6 is involved in phosphorylation of STAT3 by the overexpression of LEDGF/DFS70, mRNA production of IL-6 and gp130 in EGFP-LEDGF-HaCaT was suppressed by siRNA to IL-6 (siIL-6) and gp130 (sigp130), and then the protein levels of phosphorylated STAT3 in the cells were measured. As shown in Fig. 1c and d, both siIL-6 and sigp130 decreased phosphorylated STAT3 (p-STAT3) compared to the control (siCD4) under the diminution of each protein. Our findings provide evidence that IL-6 and gp130 are essential for the increased p-STAT3 expression that is observed in EGFP-LEDGF-HaCaT.

We have demonstrated that IL-6 expression is significantly upregulated via activation of the p38 pathway in EGFP-LEDGF-HaCaT [7]. The mechanism by which the regulatory effects of p38 are mediated involves several p38 downstream kinases, including the MAPK-activated protein kinase 2 (MK2). Thus, we investigated whether MK2 is also activated in EGFP-LEDGF-HaCaT, using Western blot analysis. As shown in Fig. 1e, the MK2 was more phosphorylated in EGFP-LEDGF-HaCaT than in EGFP-HaCaT. Furthermore, to determine whether MK2 activation is involved in the IL-6/STAT3 pathway in EGFP-LEDGF-HaCaT, protein levels of IL-6 and p-STAT3 were measured in the EGFP-LEDGF-HaCaT whose MK2 phosphorylation had been suppressed by siRNA to MK2 (siMK2). The increased expression of both the IL-6 and the p-STAT3 proteins was downregulated with siMK2 in the EGFP-LEDGF-HaCaT (Fig. 1f and g).

We studied whether excessive expression of LEDGF/DFS70 indeed results in up-regulated expression of the proinflammatory cytokines TNF-α and IFN-β1, the chemokines IL-8 and CCL5, and the KC differentiation-related genes keratin K1 and keratin K10, as occurs in psoriatic KCs. We compared their mRNA and protein expression levels with EGFP-LEDGF-HaCaT versus with EGFP-HaCaT, in both cases cultured for 24–72 h after incubation. These analyses showed that EGFP-LEDGF-HaCaT had higher mRNA expression for IL-8 (24, 48 and 72 h), TNF-α (24 and 72 h), CCL5 (24, 48 and 72 h) and IFN-β1 (24, 48 and 72 h) than EGFP-HaCaT had (Fig. 2a–d). In contrast, the mRNA expression of the KC-differentiating markers keratin K1 and keratin K10 was decreased by a factor of approximately 0.1–0.5 in EGFP-LEDGF-HaCaT compared with that in EGFP-HaCaT (Fig. 2e and f). Moreover, IL-8 protein expression was increased in EGFP-LEDGF-HaCaT compared to that in EGFP-HaCaT at 72 h after incubation (Fig. 2g). Similarly, TNF-α (Fig. 2h) and CCL5 (data not shown) proteins also increased. Although LEDGF/DFS70 was shown to be induced by TNF-α and the overexpression of LEDGF/DFS70 abolished the effect of TNF-α [10], there are no reports that overexpression of LEDGF/DFS70 induces TNF-α expression. Our findings suggest that LEDGF/DFS70 may regulate the expression of TNF-α in KCs, and it is a potentially attractive target for controlling the effect of TNF-α

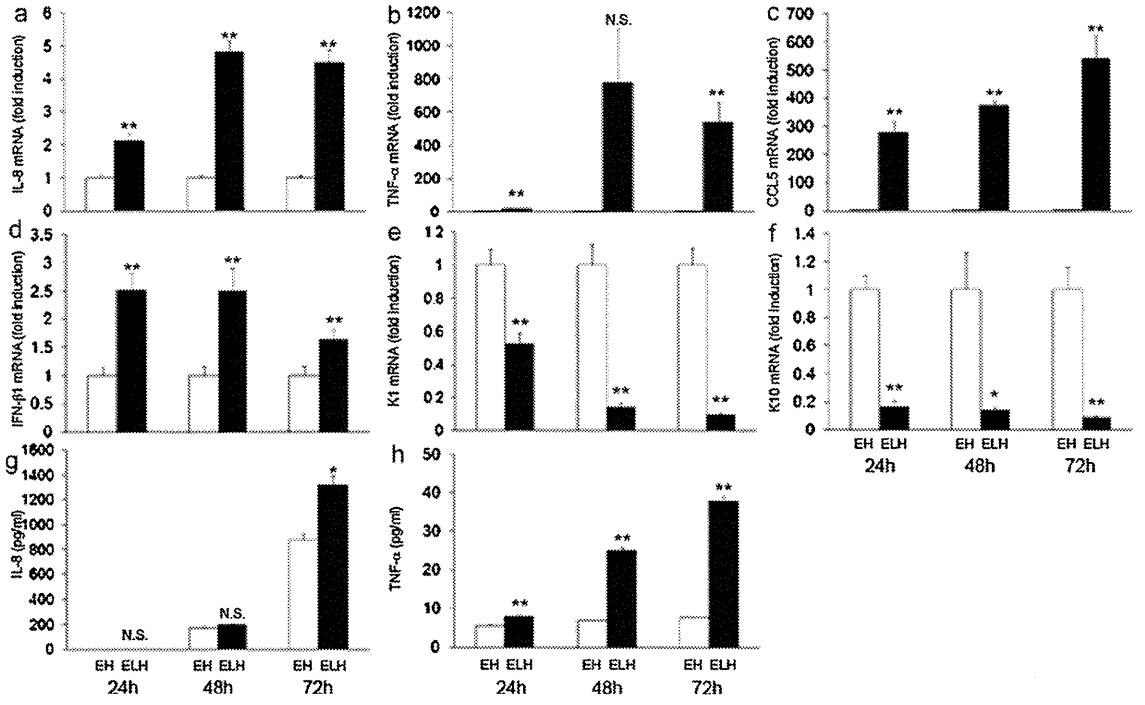

Fig. 2. qPCR and ELISA of EGFP-LEDGF-HaCaT and EGFP-HaCaT. After 24, 48 and 72 h of incubation, mRNA and protein levels in EGFP-LEDGF-HaCaT (ELH) and EGFP-HaCaT (EH) were evaluated by RT-PCR (a–f) and Western blot (g and h), respectively. RT-PCR was performed for IL-8 (a), TNF-α (b), CCL5 (c), IFN-β1 (d), K1 (e) and K10 (f). GAPDH was used to normalize the gene expression. Protein secretion levels of IL-8 (g) and TNF-α (h) were measured by ELISA. Statistical significance between groups was assessed using paired Student's *t*-test ($n = 4$). Error bars represent the SEM. N.S.: not significant. $^{*}P < 0.05$. $^{**}P < 0.01$.

In summary, we demonstrated that the MK2/IL-6/STAT3 pathway is activated in EGFP-LEDGF-HaCaT. Furthermore, we revealed that the expression of TNF-α, IL-8, CCL5 and IFN-β1 is increased and the expression of K1 and K10 is decreased in these cells. These findings suggest that LEDGF/DFS70 may play a pivotal role in activating psoriatic KCs *in vivo* via the p38/MK2/IL-6/STAT3 pathway. Because of its role as a regulator of KC differentiation, LEDGF/DFS70 is a potentially effective target for new therapies aimed at psoriasis and other proliferative diseases. We believe EGFP-LEDGF-HaCaT will be useful in the development of novel therapeutic drugs for psoriasis.

Acknowledgement

This work was supported by a Grant-in-Aid for Scientific Research, (C) 20591319 (K.S.) from the Ministry of Education, Culture, Sports, Science and Technology of Japan.

Appendix A. Supplementary data

Supplementary data associated with this article can be found, in the online version, at doi:10.1016/j.jdermsci.2011.05.004.

References

[1] Ochs RL, Muro Y, Si Y, Ge H, Chan EK, Tan EM. Autoantibodies to DFS 70 kd/transcription coactivator p75 in atopic dermatitis and other conditions. J Allergy Clin Immunol 2000;105:1211–20.
[2] Singh DP, Ohguro N, Chylack Jr LT, Shinohara T. Lens epithelium-derived growth factor: increased resistance to thermal and oxidative stresses. Invest Ophthalmol Vis Sci 1999;40:1444–51.
[3] Ge H, Si Y, Roeder RG. Isolation of cDNAs encoding novel transcription coactivators p52 and p75 reveals an alternate regulatory mechanism of transcriptional activation. EMBO J 1998;17:6723–9.
[4] Huang TS, Myklebust LM, Kjarland E, Gjertsen BT, Pendino F, Bruserud O, et al. LEDGF/p75 has increased expression in blasts from chemotherapy-resistant human acute myelogenic leukemia patients and protects leukemia cells from apoptosis in vitro. Mol Cancer 2007;31:6.
[5] Sano S, Chan KS, Carbajal S, Clifford J, Peavey M, Kiguchi K, et al. Stat3 links activated keratinocytes and immunocytes required for development of psoriasis in a novel transgenic mouse model. Nat Med 2005;11:43–9.
[6] Johansen C, Funding AT, Otkjaer K, Kragballe K, Jensen UB, Madsen M, et al. Protein expression of TNF-alpha in psoriatic skin is regulated at a posttranscriptional level by MAPK-activated protein kinase 2. J Immunol 2006;176:1431–8.
[7] Takeichi T, Sugiura K, Muro Y, Matsumoto K, Ogawa Y, Futamura K, et al. Overexpression of LEDGF/DFS70 induces IL-6 via p38 activation in HaCaT cells, similar to that seen in the psoriatic condition. J Invest Dermatol 2010;130:2760–7.
[8] Sugiura K, Muro Y, Nishizawa Y, Okamoto M, Shinohara T, Tomita Y, et al. LEDGF/DFS70, a major autoantigen of atopic dermatitis, is a component of keratohyalin granules. J Invest Dermatol 2007;127:75–80.
[9] Hughes S, Jenkins V, Dar MJ, Engelman A, Cherepanov P. Transcriptional coactivator LEDGF interacts with Cdc7-activator of S-phase kinase (ASK) and stimulates its enzymatic activity. J Biol Chem 2010;285:541–54.
[10] Takamura Y, Fatma N, Kubo E, Singh DP. Regulation of heavy subunit chain of gamma-glutamylcysteine synthetase by tumor necrosis factor-alpha in lens epithelial cells: role of LEDGF/p75. Am J Physiol Cell Physiol 2006;290:C554–566.

Takuya Takeichi
Kazumitsu Sugiura*
Yoshinao Muro
Yasushi Ogawa
Masashi Akiyama
Department of Dermatology,
Nagoya University Graduate School of Medicine,
65 Tsurumai-cho, Showa-ku, Nagoya 466-8550, Japan

*Corresponding author. Tel.: +81 52 744 2314;
fax: +81 52 744 2318
E-mail address: kazusugi@med.nagoya-u.ac.jp (K. Sugiura).

6 April 2011
doi:10.1016/j.jdermsci.2011.05.004

Hair Shaft Abnormalities in Localized Autosomal Recessive Hypotrichosis 2 and A Review of Other Non-syndromic Human Alopecias

Hiraku Suga[1], Yuichiro Tsunemi[1], Makoto Sugaya[1], Satoru Shinkuma[2], Masashi Akiyama[2], Hiroshi Shimizu[2] and Shinichi Sato[1]
Departments of Dermatology, [1]Faculty of Medicine, University of Tokyo, 7-3-1 Hongo, Bunkyo-ku, Tokyo 113-8655, and [2]Hokkaido University Graduate School of Medicine, Sapporo, Japan. E-mail: hiraku_s2002@yahoo.co.jp
Accepted December 16, 2010.

Localized autosomal recessive hypotrichosis (LAH) 2 is a type of non-syndromic human alopecia that is inherited as an autosomal recessive trait. We describe here a patient with LAH2 who had mutations in the *lipase H* (*LIPH*) gene. We analysed hair shaft morphology using light and scanning electron microscopy (SEM). In addition, we review the features of other non-syndromic human alopecias.

CASE REPORT

The patient was a 4-year-old boy, the firstborn of healthy and unrelated Japanese parents, born after an uneventful pregnancy. He had scant hair at birth, which grew very slowly in infancy.

Clinical examination revealed hypotrichosis of the scalp (Fig. 1a). The hairs were sparse, thin, and curly, and not easily plucked. The left eyebrow hair was sparse, but the eyelashes and other body hair were present in normal amounts. Teeth, nails, and the ability to sweat were completely normal. Clinical features of keratosis pilaris, milia, scarring, and palmoplantar keratoderma were absent. Psychomotor development was normal. The patient's younger brother also had severe hypotrichosis; since birth his hair was curly, and his eyebrow hair virtually absent (Fig. 1b). No other family members, including his parents, had similar hair abnormalities. Laboratory tests of the patient showed normal serum levels of copper and zinc, and liver and kidney function tests were all within normal ranges. Over a period of 2 years there was no improvement or exacerbation of hypotrichosis in the patient.

Light microscopy of the patient's scalp hairs revealed that approximately 10% had structural abnormalities. Abnormal hairs were composed of thick dark parts and thin light parts (Fig. 2a). SEM revealed alterations of the cuticular architecture. Cuticular cells were absent from both the thick and thin parts (Fig. 2b). Cross-sectional observation showed that thick, but not thin, sections had hair medulla (Fig. 2c, d). Light microscopy on hairs from the patient's younger brother revealed that they were composed of thin and thick parts (data not shown).

Based on the clinical features, hair microscopy and family pedigree, we suspected LAH2 or LAH3. To determine the type of LAH, we looked for gene mutations in *LIPH* and *LPAR6* (encoding lysophosphatidic acid receptor 6). Two prevalent missense mutations in *LIPH* were found (1); c.736T>A (p.Cys246Ser) and c.742C>A (p.His248Asn). The mutations were carried in a compound heterozygous state. No mutations were found in *LPAR6*. The parents did not consent to genetic testing of the younger brother or themselves.

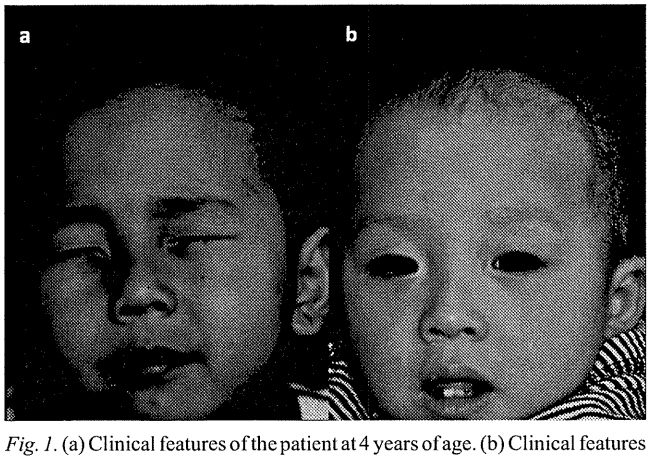

Fig. 1. (a) Clinical features of the patient at 4 years of age. (b) Clinical features of the younger brother at 1 year 4 months of age. Permission is given from the parents to publish these photos.

DISCUSSION

The different LAH subtypes map to chromosomes 18q12.1, 3q27.3 and 13q14.11–13q21.32, and are designated LAH1, LAH2 and LAH3, respectively (2–4). Mutations in *DSG4* (encoding desmoglein 4) have been found to be responsible for LAH1 (5). Kazantseva et al. (6) reported deletion mutations in *LIPH* leading to LAH2. Pasternack et al. (7) reported disruption of *LPAR6* in families affected with LAH3.

Table I summarizes of genetic, non-syndromic human alopecias. In *hypotrichosis simplex of the scalp*, hair loss

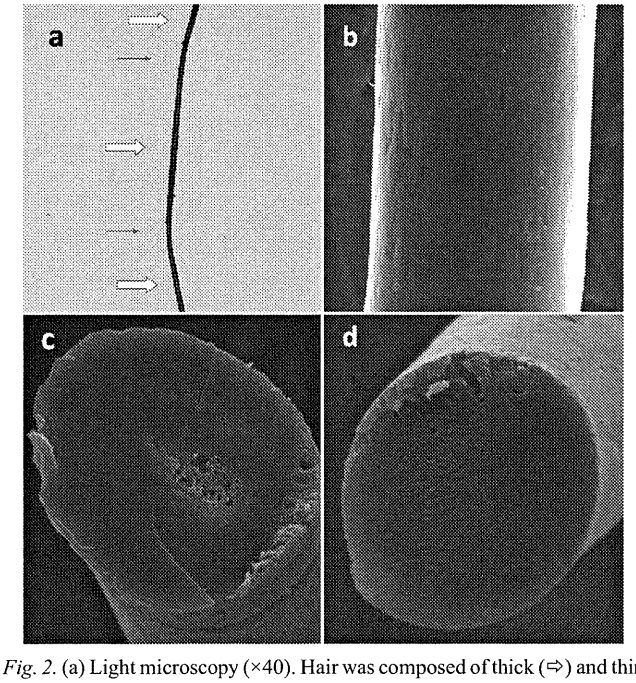

Fig. 2. (a) Light microscopy (×40). Hair was composed of thick (⇨) and thin parts (→). (b) Scanning electron microscopy (×900). Cuticular cells were absent in both thick and thin sections. (c, d) Scanning electron microscopy (cross-section, ×900). (c) Thick regions showed hair medulla, while (d) thin regions did not.

is limited to the scalp without hair shaft abnormalities. The causative gene is *CDSN* (encoding corneodesmosin) on 6p21.3 (8). The clinical presentations of *monilethrix* vary among patients. Mild cases have hair loss limited to the scalp, while severe cases show generalized alopecia. Hair shaft abnormalities are characteristic, demonstrating regularly-spaced, spindle-shaped swellings. The nodes are as thick as normal hair and the atrophic internodes represent areas where the hair is easily broken. Causative genes are *hHb1*, *hHb3* and *hHb6* (12q13) (9), which encode for basic hair keratins.

In case of *atrichia with papular lesions*, hair loss on the entire body occurs several months after birth. The gene responsible is *HR* (encoding "hairless") (10), a transcription modulating factor that influences the regression phase of the hair shaft cycle. Patients with *hypotrichosis, Marie Unna type* have hard and rough scalp hair, described as iron-wire hair. Generalized hypotrichosis is often seen. *U2HR*, an inhibitory upstream open reading frame of the human hairless gene (11), is mutated in this condition. *Hereditary hypotrichosis simplex* is characterized by hair follicle miniaturization. The defective gene is *APCDD1* (encoding adenomatosis polyposis down-regulated 1) (12). Hairs are short, thin, and easily plucked. Eyelashes and eyebrows are also affected.

As already mentioned, there are three types of *localized hereditary hypotrichosis*. LAH1 patients have hair shaft abnormalities that resemble moniliform hair (13). LAH1 can be viewed as an autosomal recessive form of monilethrix. Patients with LAH2 and LAH3 have woolly hair (14, 15), and eyelashes and eyebrows are often sparse or absent. Upper and lower limb hairs are sometimes absent too.

Our patient had hypotrichosis of the scalp with sparse left eyebrow hair and irregularly spaced segments of thick and thin hair, but not to a degree that could be labelled moniliform. The mode of inheritance was autosomal recessive and *LIPH* was found to be abnormal, thus establishing a diagnosis of LAH2. One of the mutations (c.736T>A) leads to an amino acid change (p.Cys246Ser) of a conserved cysteine residue, which forms intramolecular disulphide bonds in the lid domain in the structure model of LIPH (1). The other mutation (c.742C>A) results in alteration of one of the amino acids of the catalytic triad (Ser^{154}, Asp^{178}, and His^{248}) of LIPH (p.His248Asn) (1).

Regarding hair shaft morphology, Horev et al. (14) reported that hairs of LAH2 patients showed decreased diameter under light microscopy. This is the first report to describe hairs from an LAH2 patient by SEM. Shimomura et al. (13) observed hairs of LAH1 patients by SEM and found variable thickness of the hair shaft, resulting in nodes and internodes. Which are absent in LAH1 (our observation). Longitudinal ridges and flutes were observed at internodes, and the breaks always occurred at internodes in LAH1. These features resemble those of moniliform hair rather than LAH2. However, in the end gene analysis is probably easier to accomplish than SEM to distinguish the two types of LAH.

ACNOWLEDGEMENTS

We thank Dr Andrew Blauvelt, Department of Dermatology, Oregon Health & Science University, for many helpful comments.

REFERENCES

1. Shinkuma S, Akiyama M, Inoue A, Aoki J, Natsuga K, Nomura T, et al. LIPH prevalent founder mutations lead to loss of P2Y5 activation ability of PA-PLA1α in autosomal recessive hypotrichosis. Hum Mutat 2010; 31: 602–610.
2. Rafique MA, Ansar M, Jamai SM, Malik S, Sohail M, Faiyaz-Ul-Haque M, et al. A locus for hereditary hypotrichosis localized to human chromosome 18q21.1. Eur J Hum Genet 2003; 11: 623–628.
3. Aslam M, Chahrour MH, Razzaq A, Haque S, Yan K, Leal SM, et al. A novel locus for autosomal recessive form of hypotrichosis maps to chromosome 3q26.33-q27.3. J Med Genet 2004; 41: 849–852.
4. Wali A, Chishti MS, Ayub M, Yasinzai M, Kafaitullah, Ali G, et al. Localization of a novel autosomal recessive hypotrichosis locus (LAH3) to chromosome 13q14.11-q21.32. Clin Genet 2007; 72: 23–29.
5. Kljuic A, Bazzi H, Sundberg JP, Martinez-Mir A, O'Shaughnessy R, Mahoney MG, et al. Desmoglein 4 in hair follicle differentiation and epidermal adhesion: evidence from inherited hypotrichosis and acquired pemphigus vulgaris. Cell 2003; 113: 249–260.
6. Kazantseva A, Goltsov A, Zinchenko R, Grigorenko AP, Abrukova AV, Moliaka YK, et al. Human hair growth deficiency is linked to a genetic defect in the phospholipase gene LIPH. Science 2006; 314: 982–985.
7. Pasternack SM, von Kugelgen I, Aboud KA, Lee YA, Ruschendorf F, Voss K, et al. G protein-coupled receptor P2RY5 and its ligand LPA are involved in maintenance of human hair growth. Nat Genet 2008; 40: 329–334.

Table I. *Features of genetic, non-syndromic human alopecias*

Disease (ref)	Hair shaft shape	Eyelash/eyebrow	Causative gene	Mode of inheritance
Hypotrichosis simplex of scalp (8)	Normal	Normal	*CDSN*	Autosomal dominant
Monilethrix (9)	Regularly spaced, spindle-shaped swellings	Absent to normal	*hHb1, 3, 6*	Autosomal dominant
Atrichia with papular lesions (10)	Normal	Absent	*HR*	Autosomal recessive
Hypotrichosis, Marie Unna type (11)	Iron-wire	Sparse	*U2HR*	Autosomal dominant
Hereditary hypotrichosis simplex (12)	Short, thin, easily plucked	Absent to sparse	*APCDD1*	Autosomal dominant
Localized hereditary hypotrichosis (LAH1) (2, 5, 13)	Moniliform	Absent to normal	*DSG4*	Autosomal recessive
Localized hereditary hypotrichosis (LAH2) (3, 6, 14)	Curled	Absent to normal	*LIPH*	Autosomal recessive
Localized hereditary hypotrichosis (LAH3) (4, 7, 15)	Curled	Absent to normal	*LPAR6*	Autosomal recessive

8. Davalos NO, Garicia-Vargas A, Pforr J, Davalos IP, Picos-Cardenas VJ, Garcia-Cruz D, et al. A non-sense mutation in the corneodesmosin gene in a Mexican family with hypotrichosis simplex of the scalp. Br J Dermatol 2005; 153: 1216–1219.
9. Richard G, Itin P, Lin JP, Bon A, Bale SJ. Evidence for genetic heterogeneity in monilethrix. J Invest Dermatol 1996; 107: 812–814.
10. Ahmad W, Faiyaz ul Haque M, Brancolini V, Tsou HC, ul Haque S, Lam H, et al. Alopecia universalis associated with a mutation in the human hairless gene. Science 1998; 279: 720–724.
11. Wen Y, Liu Y, Xu Y, Zhao Y, Hua R, Wang K, et al. Loss-of-function mutations of an inhibitory upstream ORF in the human hairless transcript cause Marie Unna hereditary hypotrichosis. Nat Genet 2009; 41: 228–233.
12. Shimomura Y, Agalliu D, Vonica A, Luria V, Wajid M, Baumer A, et al. APCDD1 is a novel Wnt inhibitor mutated in hereditary hypotrichosis simplex. Nature 2010; 464: 1043–1047.
13. Shimomura Y, Sakamoto F, Kariya N, Matsunaga K, Ito M. Mutations in the desmoglein 4 gene are associated with monilethrix-like congenital hypotrichosis. J Invest Dermatol 2006; 126: 1281–1285.
14. Horev L, Tosti A, Rosen I, Hershko K, Vincenzi C, Nanova K, et al. Mutations in lipase H cause autosomal recessive hypotrichosis simplex with wooly hair. J Am Acad Dermatol 2009; 61: 813–818.
15. Horev L, Saad-Edin B, Ingber A, Zlotogorski A. A novel deletion mutation in P2RY5/LPA_6 gene cause autosomal recessive woolly hair with hypotrichosis. J Eur Acad Dermatol Venereol 2010; 24: 858–859.

THE JOURNAL OF DERMATOLOGY

doi: 10.1111/j.1346-8138.2011.01209.x

Journal of Dermatology 2011; **38**: 353–363

SPECIAL REPORT

Prevalence of dermatological disorders in Japan: A nationwide, cross-sectional, seasonal, multicenter, hospital-based study

Masutaka FURUE,[1,2]* Souji YAMAZAKI,[1] Koichi JIMBOW,[1] Tetsuya TSUCHIDA,[1] Masayuki AMAGAI,[1] Toshihiro TANAKA,[1,2] Kayoko MATSUNAGA,[1,2] Masahiko MUTO,[1,2] Eishin MORITA,[1,2] Masashi AKIYAMA,[2] Yoshinao SOMA,[2] Tadashi TERUI,[2] Motomu MANABE[2]

Scientific Committee, Japanese Dermatological Association [1](2006–2007), and [2](2008–2009), Tokyo, Japan

ABSTRACT

To clarify the prevalence of skin disorders among dermatology patients in Japan, a nationwide, cross-sectional, seasonal, multicenter study was conducted in 69 university hospitals, 45 district-based pivotal hospitals, and 56 private clinics (170 clinics in total). In each clinic, information was collected on the diagnosis, age, and gender of all outpatients and inpatients who visited the clinic on any one day of the second week in each of May, August, and November 2007 and February 2008. Among 67 448 cases, the top twenty skin disorders were, in descending order of incidence, miscellaneous eczema, atopic dermatitis, tinea pedis, urticaria/angioedema, tinea unguium, viral warts, psoriasis, contact dermatitis, acne, seborrheic dermatitis, hand eczema, miscellaneous benign skin tumors, alopecia areata, herpes zoster/postherpetic neuralgia, skin ulcers (nondiabetic), prurigo, epidermal cysts, vitiligo vulgaris, seborrheic keratosis, and drug eruption/toxicoderma. Atopic dermatitis, impetigo, molluscum, warts, acne, and miscellaneous eczema shared their top-ranking position in the pediatric population, whereas the most common disorders among the geriatric population were tinea pedis, tinea unguium, psoriasis, seborrheic dermatitis, and miscellaneous eczema. For some disorders, such as atopic dermatitis, contact dermatitis, urticaria/angioedema, prurigo, insect bites, and tinea pedis, the number of patients correlated with the average high and low monthly temperatures. Males showed a greater susceptibility to some diseases (psoriasis, erythroderma, diabetic dermatoses, *inter alia*), whereas females were more susceptible to others (erythema nodosum, collagen diseases, livedo reticularis/racemosa, hand eczema, *inter alia*). In conclusion, this hospital-based study highlights the present situation regarding dermatological patients in the early 21st century in Japan.

Key words: age, Japan, prevalence, sex, skin diseases.

INTRODUCTION

Skin forms the outermost part of the human body and it acts as a vital barrier to external and internal damage. Various external and internal stimuli, which can be either short- or long-term, can affect the homeostasis of the skin, leading to a variety of disorders. The development and perpetuation of skin disorders are multifactorial in nature, and can result from genetic, environmental, mechanical, meteorological and even cultural effects. Skin disorders therefore include a vast range of diseases.

Although it is difficult to know the exact prevalence or incidence of skin diseases, several hospital-based

Correspondence: Masutaka Furue, M.D., Ph.D., Department of Dermatology, Kyushu University, Maidashi 3-1-1 Higashiku, Fukuoka 812-8582, Japan. Email: furue@dermatol.med.kyushu-u.ac.jp

*Chair.

Received 1 September 2010; accepted 1 September 2010.

studies have shown that skin diseases are very common. Of a total of 11 191 patients seen by a general practitioner in the UK, 2386 (21%) presented dermatological complaints. Among these there was a preponderance of females (1604, 67%), and the most common skin diseases seen were viral warts, eczema and benign tumors.[1] In the Netherlands, 235–460/1000 person-years of children aged 0–17 years contacted general practitioners in 1987 and 2001,[2] and these contacts frequently involved bacterial, viral, fungal, eczematous or traumatic skin diseases.[2] Tamer *et al.* reported on 6300 pediatric cases aged 0–16 years who visited dermatological clinics in Turkey; this group showed a preponderance of bacterial, viral and eczematous skin diseases.[3] In the case of Japan, there is no authentic report in the published work on any investigation of the prevalence of skin diseases; therefore, the Japanese Dermatological Association conducted a nationwide, cross-sectional, seasonal, multicenter, hospital-based study.

METHODS

A total of 190 dermatology clinics at 76 university hospitals, 55 district-based pivotal hospitals and 59 private clinics participated in this study. At each clinic,

Table 1. Numbers of patients recruited in each season

	Number of patients				
	May 2007	August 2007	November 2007	February 2008	Total
University Hospitals $n = 69$	8558	7944	7782	7778	32 062 (47.54%)
District-based Hospitals $n = 45$	3505	3450	2890	2864	12 709 (18.84%)
Private clinics $n = 56$	5779	6709	5364	4825	22 677 (33.62%)
Total	17 842	18 103	16 036	15 467	67 448 (100%)

Table 2. Age distribution and sex difference of patients

Age distribution (years old)	Number of patients	Male patients	Female patients	Sex undescribed
0–5	4192 (6.22%)	2200 (7.12%)	1983 (5.49%)	9
6–10	2099 (3.11%)	1047 (3.39%)	1047 (2.9%)	5
11–15	1711 (2.54%)	815 (2.64%)	893 (2.47%)	3
16–20	2270 (3.37%)	995 (3.22%)	1266 (3.5%)	9
21–25	3219 (4.77%)	1245 (4.03%)	1960 (5.43%)	14
26–30	3516 (5.21%)	1378 (4.46%)	2126 (5.89%)	12
31–35	4050 (6%)	1546 (5%)	2483 (6.87%)	21
36–40	3807 (5.64%)	1604 (5.19%)	2180 (6.03%)	23
41–45	3298 (4.89%)	1387 (4.49%)	1879 (5.2%)	32
46–50	3201 (4.75%)	1326 (4.29%)	1848 (5.12%)	27
51–55	4062 (6.02%)	1763 (5.71%)	2279 (6.31%)	20
56–60	5543 (8.22%)	2503 (8.1%)	3012 (8.34%)	28
61–65	5413 (8.03%)	2533 (8.2%)	2846 (7.88%)	34
66–70	5629 (8.35%)	2775 (8.98%)	2824 (7.82%)	30
71–75	6157 (9.13%)	3195 (10.34%)	2923 (8.09%)	39
76–80	4777 (7.08%)	2487 (8.05%)	2259 (6.25%)	31
81–85	2636 (3.91%)	1297 (4.2%)	1318 (3.65%)	21
86–90	1098 (1.63%)	508 (1.64%)	583 (1.61%)	7
91–100	427 (0.63%)	166 (0.54%)	259 (0.72%)	2
≥101	16 (0.02%)	3 (0.01%)	2 (0.01%)	11
Age undescribed	327 (0.48%)	126 (0.41%)	155 (0.43%)	46
Total	67 448 (100%)	30 899 (100%)	36 125 (100%)	424

information on diagnosis, age and sex was collected from all outpatients and inpatients who visited the clinics or who were hospitalized on any single day of the second week in each of May, August and November 2007 and February 2008. Reports on the monthly average values of the high and low temperatures and humidities were collected from the Meteorological Agency. The information on 67 448 cases from 170 clinics (69 university hospitals, 45 district-based pivotal hospitals and 56 private clinics) that participated in all of the four seasonal examinations was analyzed. Statistical analyses were performed by using Spearman's rank correlation coefficient. A P-value of <0.05 was considered to be statistically significant. This study was approved by the internal ethical review boards of the Japanese Dermatological Association.

Table 3. Prevalence of skin diseases in 67 448 patients

Burn	899 (1.33%)	Syphilis	24 (0.04%)
Trauma	409 (0.61%)	Miscellaneous sexually transmitted diseases	41 (0.06%)
Skin ulcer (nondiabetic)	1334 (1.98%)		
Pressure ulcer	608 (0.9%)	Bullous pemphigoid	510 (0.76%)
Miscellaneous physico-chemical skin damage	681 (1.01%)	Pemphigus	424 (0.63%)
		Miscellaneous bullous diseases	141 (0.21%)
Diabetic dermatoses	436 (0.65%)	Systemic sclerosis	619 (0.92%)
Atopic dermatitis	6733 (9.98%)	Systemic lupus erythematosus	525 (0.78%)
Hand eczema	2024 (3%)	Dermatomyositis	304 (0.45%)
Contact dermatitis	2643 (3.92%)	Miscellaneous collagen diseases	915 (1.36%)
Seborrheic dermatitis	2213 (3.28%)	Anaphylactoid purpura	171 (0.25%)
Miscellaneous eczema	12590 (18.67%)	Reticular/racemous livedo	81 (0.12%)
Urticaria/angioedema	3369 (4.99%)	Miscellaneous vasculitis/purpura/ circulatory disturbance	632 (0.94%)
Prurigo	1229 (1.82%)		
Drug eruption/toxicoderma	1018 (1.51%)	Mycosis fungoides	427 (0.63%)
Psoriasis	2985 (4.43%)	Miscellaneous lymphomas	285 (0.42%)
Palmoplantar pustulosis	832 (1.23%)	Pigmented nevus	709 (1.05%)
Miscellaneous pustulosis	172 (0.26%)	Seborrheic keratosis	1095 (1.62%)
Lichen planus	200 (0.3%)	Soft fibroma/acrochordon	231 (0.34%)
Miscellaneous inflammatory keratotic disorders	241 (0.36%)	Epidermal cyst	1194 (1.77%)
		Lipoma	173 (0.26%)
Tylosis/clavus	917 (1.36%)	Dermatofibroma	111 (0.16%)
Ichthyosis	61 (0.09%)	Miscellaneous benign skin tumors	1666 (2.47%)
Miscellaneous keratinization disorders	502 (0.74%)	Actinic keratosis	261 (0.39%)
Ingrown nail	597 (0.89%)	Basal cell carcinoma	324 (0.48%)
Miscellaneous nail disorder	397 (0.59%)	Squamous cell carcinoma/Bowen's disease	455 (0.67%)
Alopecia areata	1653 (2.45%)		
Androgenic alopecia	210 (0.31%)	Paget's disease	224 (0.33%)
Miscellaneous skin appendage disorders	266 (0.39%)	Malignant melanoma	808 (1.2%)
Scabies	98 (0.15%)	Miscellaneous malignant skin tumors	534 (0.79%)
Insect bite	762 (1.13%)	Vitiligo vulgaris	1134 (1.68%)
Tinea pedis	4379 (6.49%)	Chloasma/senile freckle	336 (0.5%)
Tinea unguium	3231 (4.79%)	Miscellaneous pigmented disorders	154 (0.23%)
Miscellaneous tinea	610 (0.9%)	Erythema multiforme	197 (0.29%)
Candidiasis	408 (0.6%)	Erythema nodosum	111 (0.16%)
Miscellaneous mycosis	211 (0.31%)	Miscellaneous disorders with erythematous plaques	130 (0.19%)
Acne	2430 (3.6%)		
Impetigo contagiosum	507 (0.75%)	Nevus/phacomatosis (other than pigmented nevus)	267 (0.4%)
Folliculitis	755 (1.12%)		
Erysipelas	81 (0.12%)	Rosacea/rosacea-like dermatitis	150 (0.22%)
Cellulitis	594 (0.88%)	Granulomatous diseases	192 (0.28%)
Miscellaneous bacterial infection	914 (1.36%)	Keloid/hypertrophic scar	186 (0.28%)
Molluscum contagiosum	604 (0.9%)	Cheilitis/angular cheilitis/mucous membrane diseases	95 (0.14%)
Herpes simplex	691 (1.02%)		
Herpes zoster/zoster-associated pain	1609 (2.39%)	Erythroderma	63 (0.09%)
Viral wart	3028 (4.49%)	Other diseases	666 (0.99%)
Miscellaneous viral disorders	353 (0.52%)	Total	67 448 (100%)